Phosphate and Phosphonate Derivatised Wells-Dawson Polyoxometalates as novel precursors for organic-inorganic hybrid materials

Final Degree Project

Carla Martí Torrell

Supervised by **Dr Graham Newton** (visiting university supervisor) and **Prof Maria Elena Fernández Gutiérrez** (home university supervisor)

GRAU DE QUÍMICA

UNIVERSITAT ROVIRA i VIRGILI

Tarragona, 2017

Abstract

This project aims to report a novel synthetic route to create inorganic hybrid materials based on phosphate and phosphonate groups linked to a Wells-Dawson lacunary polyoxometalate. These building blocks are aimed to serve as starting materials for further organic functionalisation. Until now the method commonly used for the synthesis of covalently bounded organic-inorganic hybrid polyoxometalates entailed firstly making the organic ligand, secondly linking it to the heteroatom that would act as an anchoring point and finally grafting the organic fragment to the lacunary polyoxometalate. By following this new approach, several synthetic drawbacks can be avoided such as the long-step synthesis of organic ligands and low yields.

This project will initially focus on the synthesis of the Wells-Dawson heteropolyoxometalate as well as its analogous lacunary structure in order to further functionalise it and obtain the phosphonate and phosphate hybrids. Comparison of their properties will also demonstrate how these novel precursors may be much more convenient in terms of redox photocatalysis and other applications.

Despite polyoxometalate species being described as early as the nineteenth century, their long lasting interest is partly based on their interesting physical and chemical properties and the large domains of applications that arise from them.

Acknowledgements

This Final Degree Project has been carried out as part of an Erasmus+ academic stay between my home university, Universitat Rovira i Virgili in Tarragona and the visiting institution, University of Nottingham in Nottingham.

This project would not have been possible without the kind support and help of many individuals. I would like to extend my sincere thanks to all of them.

I am highly indebted to Dr Graham Newton for embracing me in his research group and giving me the golden opportunity to do this research on polyoxometalates. I really appreciate his guidance and constant supervision as well as his support in completing the project.

I would like to express my special thanks of gratitude to Dr Katharina Kastner and Alexander Kibler for helping me in doing a lot of the research and teaching me so many new things, I am really thankful to both of them.

I would also like to express my gratitude towards all my laboratory mates for their kindness and willingness.

My thanks and appreciations also go to my family and friends for their unconditional support and encouragement which helped me in completion of this project, despite from the distance. And especially to Òscar, for his unconditional support in this project and always.

Table of contents

1. Objectives

The study reported in this project aimed to fulfil several objectives:

- To synthesise phosphate and phosphonate inorganic hybrid polyoxometalates following a brand new synthetic approach
- To compare the inorganic hybrid polyoxometalates' properties to those from their precursors, that is, the Wells-Dawson heteropolyoxotungstate and its analogous lacunary structure
- To evaluate the phosphorous reactivity from the phosphate group in a polyoxometalate environment towards further organic functionalisation

2. Introduction

2.1. Polyoxometalates

Polyoxometalates (commonly referred to as POMs) are discrete anionic transition-metal-oxide clusters that span a great diversity of sizes and shapes. These clusters exhibit excellent stability, solubility in both aqueous and organic media – depending on the counter cation – and a wide range of potential compositions and structures.[1]

POMs are built from the connection of metal oxides $\{MO_X\}$ polyhedral, M being typically a d-block element such as vanadium, niobium, molybdenum, tantalum and tungsten, all of them in d_0 or d_1 electronic configurations which means having a high or highest oxidation state.[2] These possess the combination of favourable ionic radii, high charge and accessibility to empty d-orbitals allowing for metal-oxygen π-bonding.[3]

POMs are built through corner sharing and edge sharing of bipyramidal MO_5 oxides and octahedral MO_6 to form extended structures. Face sharing may also occur but this is less common due to stability issues.[4] These oxide units can combine in many different ways though the most common structures are the Keggin and the Wells-Dawson (**Fig. 1**)[5].

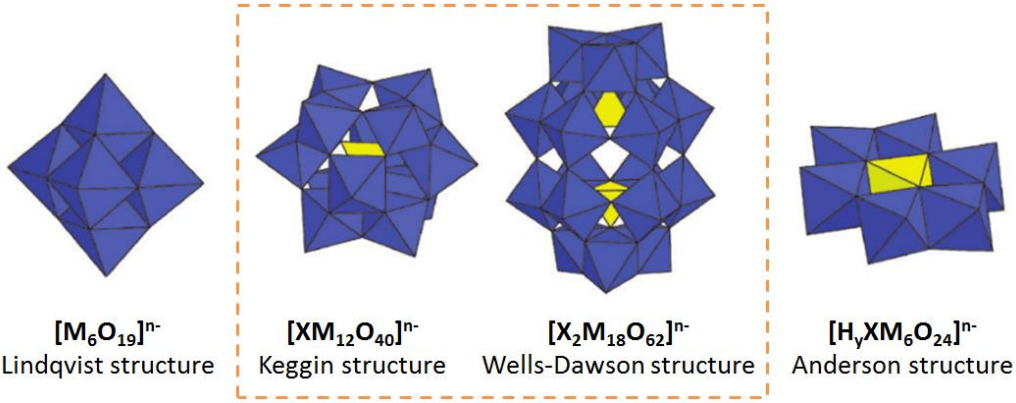

Figure 1. Most common POM structures in polyhedral representation. Colour code: MO_6 octahedral in blue, XO_n polyhedral in yellow.

POMs of molybdenum (VI), tungsten (VI) and vanadium (V) are common[6] whereas those of tantalum (V) and niobium (V) are known but synthesised far less easily.[7] Tungsten-based POMs are especially important for their ease of functionalisation and play a prominent role in the chemistry of POMs.

2.1.1. Classification of POMs

The family of POMs can be divided in two main subclasses, namely, isopolyoxometalates and heteropolyoxometalates.[8] As this project is going to focus on polyoxotungstates, the classification is going to pertain to this metal.

While isopolytungstates $[W_nO_m]^{p-}$ are only formed by metal tungsten atoms and oxo anions, heteropolytungstates $[X_zW_nO_m]^{q-}$ additionally feature heteroatoms, such as phosphorous or silicon. Examples of the isopolytungstate structure are the Lindqvist structures whereas the Keggin and the Wells-Dawson encapsulate template tetrahedral oxoanions, either $[SiO_4]^{4-}$, $[PO_4]^{3-}$ $[SO_4]^{2-}$.[9]

2.1.2. Properties of POMs

Catalytic properties

Polyoxometalates have gained increasing interest due to their catalytic properties. They have a wide range of highly stable redox states which can be accessed electrochemically, photochemically or by using reducing agents.[10] Many of the POMs can undergo successive one and two-electron reversible reductions, producing species which are electroactive.

Nevertheless, POMs not only perform well in as redox catalysts but they are seen as multifunctional catalysts due to their numerous active sites. It is reported that the surrounding protons encourage acid-catalysed reactions. [11] Moreover, the oxygen atoms at the surface of the framework possess a high negative charge, this means that oxygen sites are capable of behaving as bases and reacting with protons, thus act as active sites for base-catalysed reactions.

Stability

Polyoxometalates commonly possess high thermal, structural and oxidative stability in the solid state and in solution. This high stability is closely related to their purely inorganic nature, with no carbon atoms present which are known to be sensitive to degradation under different conditions.[12] Nevertheless, one downside is the hydrolytic stability of many species, only being stable under certain pH windows. For instance, 12-

phosphotungstic acid ($H_3PW_{12}O_{40}$) is only present at pH range 1-3.5, and only at range 1-2.2 is it free from other condensation products such as $[PW_{11}O_{39}]^{7-}$ and $[P_2W_{21}O_{71}]^{6-}$.[13]

Electronic properties

Polyoxometalate clusters are able to absorb ultraviolet light ad become photoexcited through ligand to metal charge transfer (LMCT) which involves the transferral of an electron from the doubly occupied HOMO of a terminal double-bonded oxygen to the unoccupied LUMO of the d_0 metal centre. These radical excited species perform better as redox agents than the ground state species.[2] However, hybrid POMs perform much better in this respect and thus, this property will be further explained later on.

Polyoxometalates redox capabilities are attributed to the high number of d_0 metal ions within the structure which are capable of accepting electrons in a redox process. The heteropolyanions undergo several rapid one and two-electron reversible reductions to produce the so-called *heteropoly blues*, and further irreversible multielectron reductions with simultaneous decomposition. The electrons are accepted by the metal atoms of the Keggin and Wells-Dawson heteropolyanions. If the metal atoms are all identical, the electrons are delocalised throughout the ion oxide framework at room temperature by rapid electron hopping, this is known as intervalence charge transfer. The reduction increases the negative charge density at the POM and thus their basicity. As a consequence, the reduction can be accompanied by protonation depending on the pK_a of the polyoxometalate.[14] Consequently, POMs can act in a bifunctional manner as electron/proton reservoirs.

2.1.3. Applications

Polyoxometalates play a prominent role in various areas ranging from catalysis[11,15], medicine[16], electrochemistry[17], photochemistry[18,19], water treatment[20] and magnetism[21]. This palette of applications is due to the combination of their intrinsic properties such as redox properties, large size and mass, high negative charges, nucleophilicity, electron and proton transfer/storage abilities, thermal stability and so on.

In catalysis, these species can act as effective redox catalysts, electron reservoirs and electron transfer agents. Mizuno *et al.* reported the epoxidation of olefins with hydrogen

peroxide catalysed by polyoxometalates. The versatility, accessibility and tunability of polyoxometalates opened up the development of effective epoxidation systems. In the report, two types of polyoxometalates for H_2O_2-based epoxidation are described, being catalyst precursors of polyoxotungstate or peroxomolybdate species and oxidatively and hydrolytically stable transition-metal-substituted polyoxometalates. Thanks to lacunary polyoxotungstates, the group made it possible that a broad range of olefins were epoxidised under mild conditions with high catalytic activity, selectivity and efficiency.[22] Sastry *et al.* also reported a catalytic application of the reduced Keggin ion as a switchable reducing agent in the formation of stable gold nanoparticles capped by the Keggin ions.[10]

Regarding the medicinal field, despite the numerous POMs prepared and evaluated it was unfortunate that the first POM used *in vivo*, HPA-23, was acutely toxic and thus, this discouraged biological research on these clusters. Nevertheless, literature is currently increasing exponentially in this area. POM chemotherapeutic agents have been discovered and the toxicity problems exhibited by HPA-23 are almost non-existent. Other POMs structures have also been proved to be antiviral not just *in vitro* but also *in vivo* against HIV (human immunodeficiency virus). One mode of action involves POMs inhibiting the binding of HIV gp120[a] to CD4 receptor found in the surface of immune cells and consequently also hindering the fusion of the viral with the host cell membrane. Another mode of action is the inhibition of HIV-1 reverse transcriptase.[16]

Within the photochromism field, polyoxometalates themselves do not exhibit great performance as they are not highly sensitive to light radiation. Nevertheless, what is most remarkable is the behaviour of hybrid organic-inorganic materials based on polyoxometalates clusters with greatly improved photochromic properties thanks to the charge transfer phenomenon that occurs between the organic moiety and the inorganic cluster. Some of these hybrids, especially the molybdenum-based ones, exhibit good photochromic reversibility and thus have potential applications in reusable information storage media, data display, optical signal processing, chemical switch for computers…

[a] HIV gp120 stands for an envelope glycoprotein exposed on the surface of the HIV. It is essential for virus entry into cells as it plays a vital role in attachment to specific cell surface receptors.

These materials can also be used as the reagents for photoresistance and camouflaging materials.[23]

Polyoxometalates chemistry has also been remarkable in the magnetism field. It can be employed to form different types of triangular-based spin arrays that are key to spin frustration. Magnetic spin frustration describes a situation in which a set of physical variables is incompatible with its spatial or connectivity constraints, which in this case are defined by the interaction between spin centres – usually paramagnetic transition metal ions – that can compete with each other.[24] In addition, as POMs can be reversibly reduced to mixed-valence species by injection of variable numbers of electrons, these extra electrons are delocalised over a significantly large number of centres of the framework. Consequently, the further introduction into these structures of paramagnetic metal atoms leads to the creation of clusters in which localised magnetic moments and delocalised electrons can coexist and interact. These features are motivating the development of new theoretical models in order to treat the problem of the electron transfer effects in large clusters, as well as to understand the interplay between electron delocalisation, magnetic interactions and Coulomb repulsions in high nuclearity multielectron systems.[21]

Heteropolyanions have some very useful and interesting features in electrochemical processes as well. Such properties include high stability of most of their redox potentials by changing the heteroatoms and/or the *addenda* atoms without affecting their structure, the variability of the transition metal cations which can be incorporated into the heteropolyoxometalate structure and the possibility of multiple electron transfer. These properties make heteropolyanions, especially Keggin and Dawson-type, attractive as redox catalysts for indirect electrochemical processes. Moreover, POMs have the potential to be highly selective and long-time stable redox catalysts.[14]

2.2. Hybrid materials based on polyoxometalates

The ability to combine, in a single material, inorganic and organic components at the molecular or nanometer level represents an exciting direction in material science with extraordinary implications for developing novel multifunctional materials. These inorganic/organic hybrids have the possibility to possess the advantages of both

inorganic (high strength, thermal stability, chemical resistance…) and organic (light weight, flexibility, versatility…) materials.[23]

POMs are usually chosen as building units for these kinds of novel hybrids because of their well-defined and diverse structures and well-documented reactivity. Consequently, they offer a perfectly adapted platform for a controlled localisation of the functionalisation by organic groups. A challenging aim is also to be able to form unsymmetrically functionalised structures in which two different organic groups are selectively grafted on various parts of the POM.[1]

The main goal for the hybridisation is to induce and/or increase a synergy between the two components, namely, the organic moiety and the POM and benefit from the intrinsic physicochemical properties of the POMs whilst selecting appropriate organic groups to enhance other properties. For instance, it is possible to use fully conjugated organic ligands to favour electronic transfer[25] or to insert an alkyl chain of variable length to bring flexibility to the structure.

Functionalization via covalent grafting of organic functions allows one to tune the redox, acid–base properties and the solubility of polyoxometalates, to enhance their stability and biological activity, reduce their toxicity and to facilitate their implementation in extended structures and functional devices.[5]

To summarise, the most promising route to the integration of POMs into functional architectures and devices rests on inorganic/organic hybrids.

2.2.1. Classification

Since the development of organic-inorganic hybrids, two classes of composites have emerged according to the nature of the interaction between the organic and the inorganic parts.[1]

- Class I encompasses all the systems where no covalent bonds are shared between the organic and the inorganic moieties but only electrostatic interactions, hydrogen bonds or Van der Waals interactions

- Class II describes those materials in which both parts are linked via strong covalent or ionic-covalent bonds

The anionic character of POMs naturally allows their association with organic counter cations into class I hybrids. Whilst with class II hybrids, the organic ligand needs to substitute an oxo group of the POM's structure and be directly linked to the metallic centre. The nucleophilic character of the oxygen atoms localised on the surface of the POM can also lead to covalent interactions with electrophilic groups – such as phosphates or siloxanes – bearing organic groups.[1]

This project will focus on a couple of class II hybrids which aim to covalently be linked to organic moieties via a p-block element, in particular, phosphorous.

2.2.2. The anchorage point in class II hybrids

Grafting an organic fragment onto an inorganic system requires an anchorage point ensuring the link between the two parts. This link is closely dependent on the chemical nature and electronic properties of the POM, for instance, the presence of the negative charge borne by the inorganic structure needs to be considered for suitable linkage. [1]

An essential step previous to the functionalisation is the formation of the lacunary structure. These species are formed by the removal of one or more metal oxide units from the corresponding tungsten oxide cluster (**Fig. 2**). By the controlled addition of base to the solution of POM anions, free binding sites can be generated.

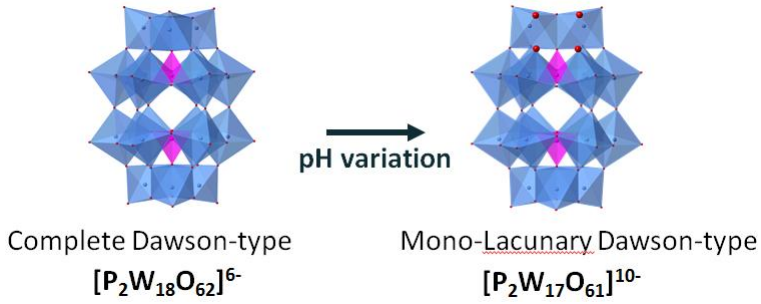

Figure 2. Synthesis of Wells-Dawson lacunary POM. The vertexes of the octahedral units represent oxygen atoms whilst the centre represents tungsten atoms. Purple tetrahedral units have phosphorous atoms in the centre.

The functionalisation of POMs through oxygen atoms located at the periphery of the structure or using a p-block element are the most conventional routes although many other coordination modes have been developed for the coordination of an organic ligand (**Fig. 3**).

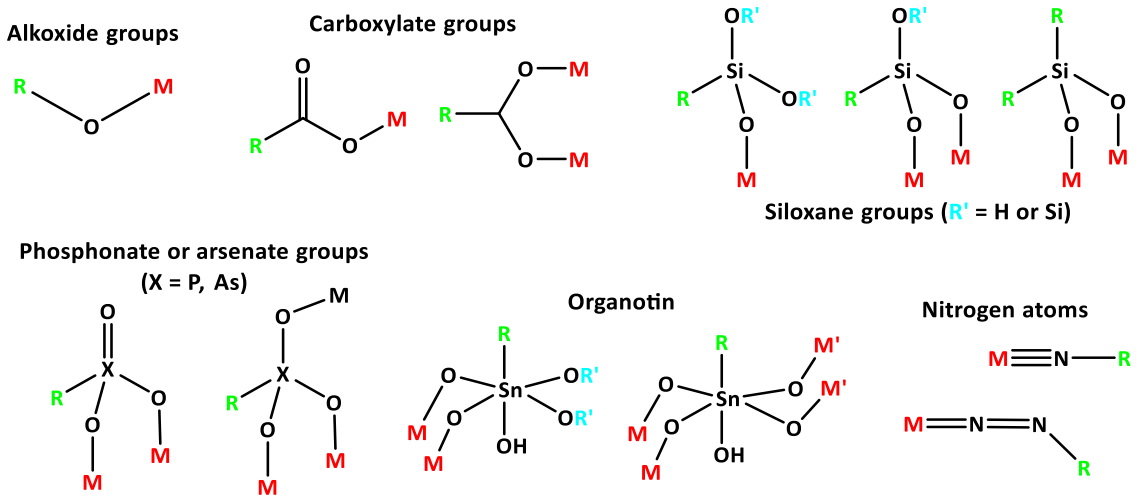

Figure 3. Coordination modes of organic ligands covalently linked to POM units *via* p-block atoms

2.2.3. Enhanced properties of hybrid POMs: Photochromism

The word *photochromism* refers to a phenomenon that the material can change colour in a reversible way by electromagnetic radiation (ultraviolet, visible or infrared illumination). The reverse process can occur by exposure to the light at a different frequency, by heating in the dark, by electrochemical polarization or by chemical oxidation. Photochromic materials exhibit a wide range of optical properties that make them attractive for a plethora of applications. For instance, the sensitivity of these materials towards light radiation makes them useful for self-developing photography, protective materials, dosimetry and actinometry.

As stated above, non-hybrid polyoxometalates do not exhibit notable photochromism compared to that of their hybrid materials, as these last ones possess the enhanced properties of both inorganic and organic materials. The enhanced photochromism observed in organic-inorganic hybrid POMs is due to the charge transfer (CT) between both organic and inorganic moieties.

Ground state POMs are characterised by intramolecular oxygen-to-metal (O → M) charge transfer bands that appear in the UV-Vis range of the light spectra. This type of charge

transfer is ligand-to-metal (LMCT) and is possible because of the d_0 electronic configuration of the metallic atoms in oxidised POMs.

When hybrid materials based on POMs are irradiated with UV light, electrons are excited from the low energy electronic states, which are mainly comprised of oxygen *2p* doubly-occupied bonding orbitals in POM (HOMO), to the high energy states, which are mainly comprised of metal *d* anti-bonding orbitals (LUMO) (**Fig. 4**)[19]. Consequently, the metal ions have d_1 instead of d_0 electronic configurations and the electrons added to polyanions have a thermally activated delocalisation within the structure.[26]

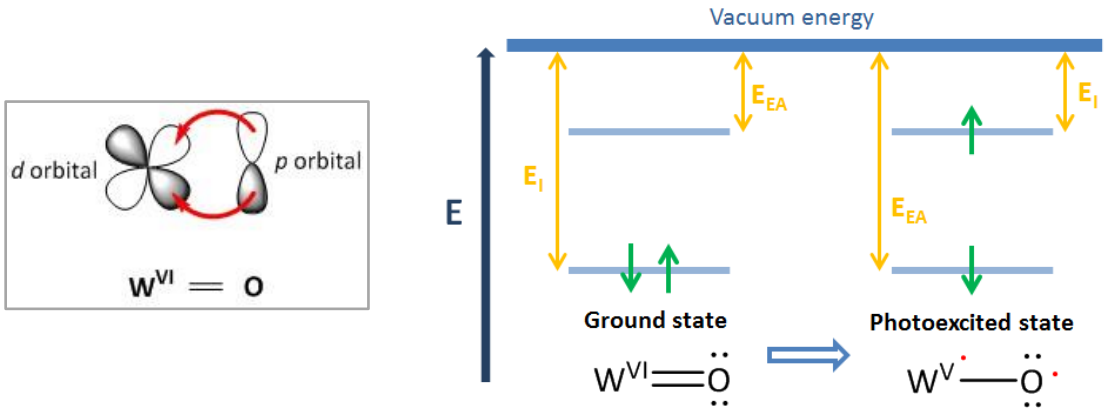

Figure 4. Simplified orbital diagram illustrating the ground state and excited state orbital occupation: photoexcitation results in the promotion of an electron from a bonding to an antibonding orbital (LMCT). The resulting excited species features lower ionisation energy (E_I) and higher electron affinity (E_{EA}) than the ground state species and is therefore both, a better oxidising agent and a better reducing agent, than the ground state species.

The band gap of POMs consists of well-defined HOMO and LUMO gap which inhibits the recombination of excited electrons and holes formed *via* the photoexcitation. Therefore, these photo-active charged species are capable of initiating chemical reactions under mild conditions.

Once photoexcited, polyoxometalates can be photochemically reduced to form coloured mixed-valance species, commonly navy blue (**Fig. 5**), while retaining the structural integrity resulting in species that are reversibly chemically active.

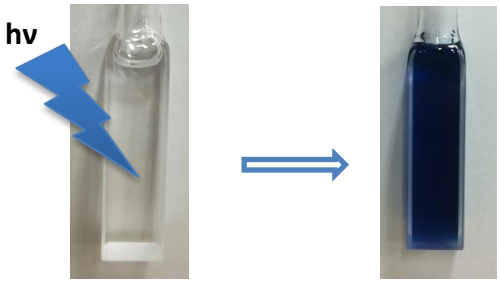

Figure 5. Photoreduction of a $2.0 \cdot 10^{-4}$ M $K_5H[P_2W_{17}O_{57}(PO_5H_5C_7)_2]$ sample in DMF under a Xe lamp (190-1000 nm) as the light source

As previously mentioned, reduction of POMs (**Fig. 6**) results in a decrease of the O → M charge transfer bands and a formation of *d-d* transitions and/or intervalence charge transfer (IVCT) bands between the neighboured metal centres with different valence states. These absorption bands are located in the visible and near infrared region. The intensity and position of the bands are approximately proportional to the number of trapped electrons.[27]

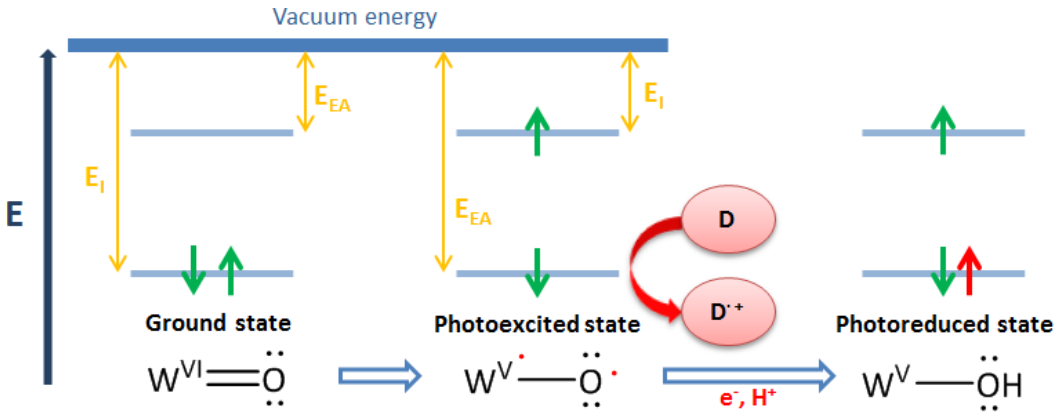

Figure 6. Simplified orbital diagram illustrating the photoreduction phenomenon carried out by a reducing donor agent (D)

The photochromic products may be different when the POMs are combined with different kinds of organic molecules. The most usually selected ones are based on organic amines, with *p* electrons, or polymers. If there is hydrogen bond present between the oxygen of POM and the hydrogen of organic moiety, such as in the case of alkyl ammonium based hybrids, the photoexcitation of O → M LMCT bands induces transfer of a proton from a hydrogen bonded atom in organic, such as alkyl ammonium nitrogen, to

a bridging oxygen atom at the photoreducible site in edge-sharing MO_6 octahedral lattice (**Eq. (1)**).

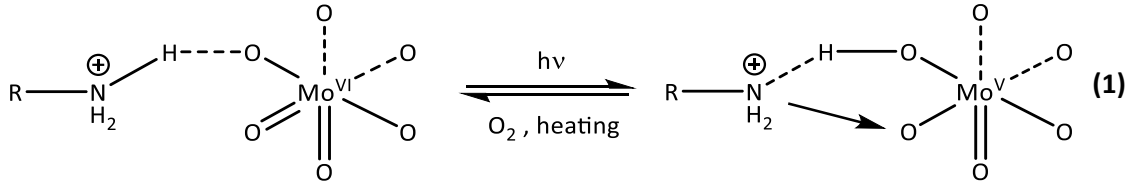

(1)

The proton transferred to the oxygen atom interacts with the d_1 electron of metal atom. Meanwhile, the hole left at the oxygen atom as a result of the O → M LMCT transition interacts with non-bonding electrons of the nitrogen atom to form a CT complex, resulting in separation of electrons and holes produced by O → M LMCT transition in the POM lattice and thus leading to the stabilisation of the coloured state. In such a case, the hydrogen bond and proton transfer are crucial for the photochromic process.

The organic molecules may not only serve as the proton donor for the coloration and stabilisation of hybrids, but also as the electron donor for the formation of coordination bond in the photoinduced CT complex.

2.2.4. Applications of hybrid POMs

The structure and properties that can be obtained for such hybrid materials depend on the nature of both components, and the search of multifunctional devices is often evoked as a motivation for their synthesis.

In the field of catalysis, the study of organic-inorganic hybrids with POMs can help to understand the interactions between organic molecules and the surface of oxides and lead to more efficient recyclable multifunctional catalysts.

In materials chemistry hybrid POMs can be linked together, they can also be incorporated into polymers, and they can interact with metallic surfaces or nanoparticles.[1] For instance, Maata *et al.* and Peng *et al.* designed hybrid organic/inorganic polymers bearing POMs as pendant groups using monosubstituted organoimido derivatives of the isopolyanion $[Mo_6O_{19}]^{2-}$ *via* conventional free-radical induced copolymerisation.[25,28] Depending on the properties of the organic moieties

different features are provided to the polymer such as extra flexibility or enhanced electronic transfer.

Other applications also involve the medicinal field. Lalot *et al.* synthesised a hybrid hydrogel with peculiar swelling properties from acrylamide and a tetrafunctionalised polymerisable heteropolyoxotungstate as cross-linker, for applications that benefit from the enhanced ability of the hydrogel to absorb water.[29]

3. Fundamentals

3.1. Synthesis of heteropolyoxotungstates and lacunary analogues

Different polyoxotungstates are obtained by self-assembly reactions[5] of the tetrahedral oxide precursors, which in this case are sodium tungstate units, commonly carried out in aqueous environments, and with the structure formed being strongly influenced by the pH of the media and presence of heteroatoms (**Fig. 7**). P-block elements such as phosphorous and silicon in a tetrahedral oxide environment are the common templates that enable the assembly of the structure, these units being encapsulated by a cage.[9]

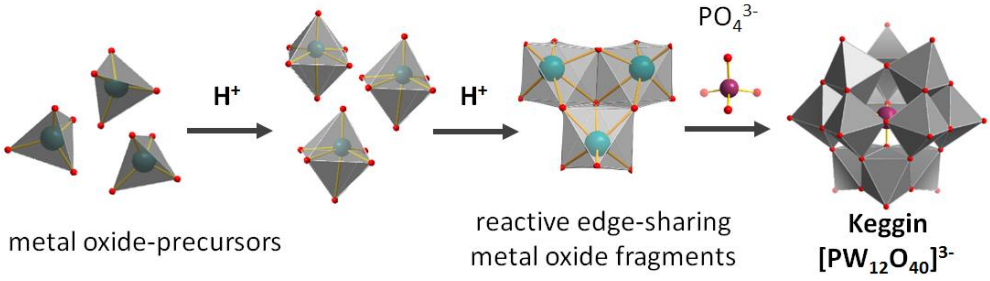

Figure 7. Synthesis of the Keggin heteropolytungstate anion. Colour code: blue spheres are tungsten atoms, red spheres are oxygen atoms and the purple ones stand for phosphorous.

As stated above, it is imperative to create the lacunary species in order to obtain a platform for further functionalisation. This modification of the structural framework of POMs involves removal of W^{VI} centres from the cage, along with their terminal oxo groups, $[WO]^{4+}$ units, to generate defect structures.[9] This process is carried out by the addition of a base to the aqueous solution of the heteropolytungstate so that a vacancy – or more than one – is generated and consequently, the organic ligand can be linked to the POM structure, with a heteroatom always bridging the organic and inorganic functions (**Fig. 8**).

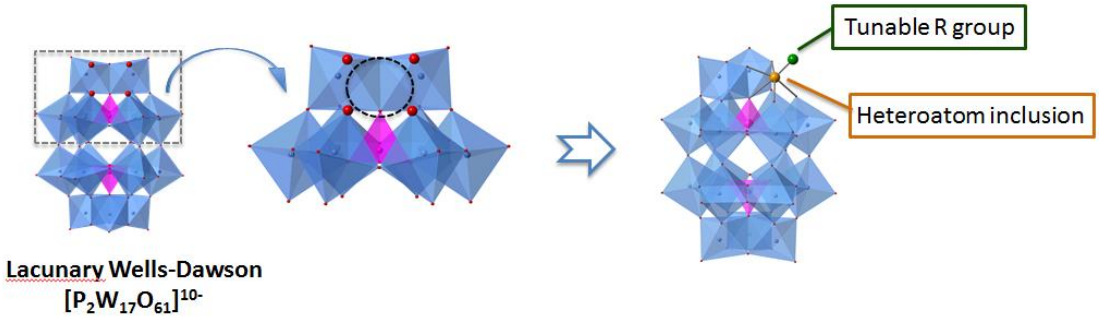

Figure 8. Lacunary Wells-Dawson POM that enables the organofunctionalisation by the inclusion of a p-block heteroatom

The reason why the formation of lacunary POMs is needed in order to further functionalise is that complete (plenary) POMs are usually weakly basic and nucleophilic. Instead, lacunary POMs have higher charges, hence increased basicity and nucleophilicity than their parent complete species. Thus they react quite easily with a variety of electrophilic groups both in water and in non-aqueous solvents. [5]

3.2. This project

The typical approach for the synthesis of hybrid organic-inorganic polyoxometalates involves two main blocks as starting materials. On one hand, the organic moiety which has previously been linked to a template oxoanion group that will act as an anchorage point. And on the other hand, the lacunary polyoxometalate cluster. With the appropriate pH and media conditions, the hybrid is generated.

For instance, Newton *et al.* studied the synthesis of $K_5H[P_2W_{17}O_{57}(PO_5H_5C_7)_2]$ in which the starting materials were the lacunary Wells-Dawson heteropolyoxotungstate and the organic ligand, which in this case was benzoic acid (bza) linked to a phosphonic group as the anchorage point for the organofunctionalisation (**Fig. 9**).[b]

[b] Manuscript in preparation. Non-published yet.

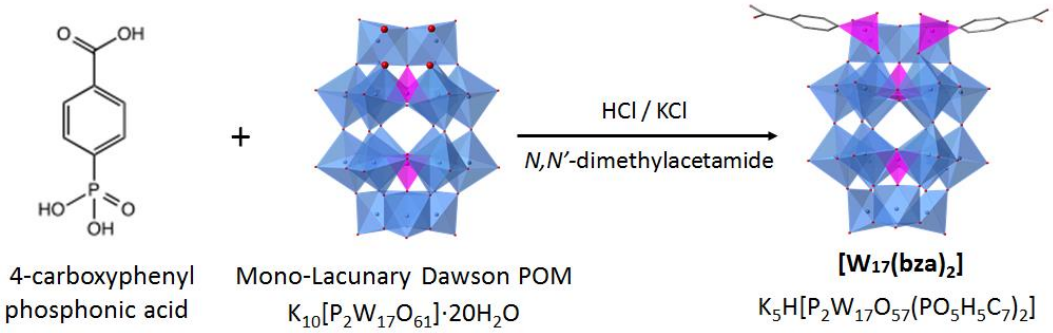

Figure 9. Synthesis of $K_5H[P_2W_{17}O_{57}(PO_5H_5C_7)_2]$ hybrid heteroPOM.

Nevertheless, this approach is not always successful. In so many cases, the yields end up being low due to difficulties when grafting the anchorage group with the organic moiety to generate the ligand. Moreover, sometimes these reactions require harsh conditions.

This project aims to describe a new approach for inorganic hybrids synthesis in order to serve as an alternative to those previously described. This new way of syntheses involves firstly the linkage of the lacunary Wells-Dawson heteropolyoxotungstate with an inorganic group, phosphate and phosphonate, which may serve as anchorage point for further functionalisation, though this last part will not be studied in this project (**Fig. 10**).

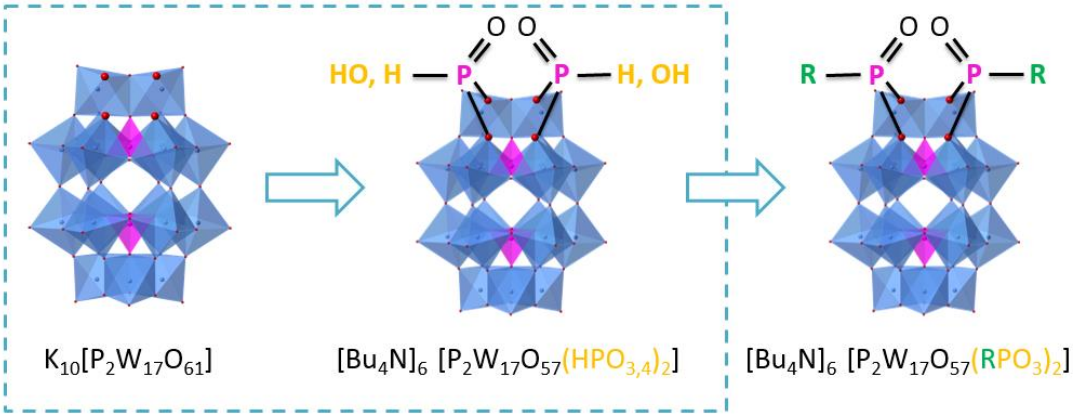

Figure 10. New approach of functionalisation of a Wells-Dawson polyoxotungstate.

4. Experimental work

4.1. Reagents and solvents

Solvents and reagents were purchased from Sigma Aldrich, Fischer Scientific, Merck Millipore, Alfa Aesar and VWR Chemicals, and used without further purification.

In the following **Table 1**, reagents used in this project are named as well as their purity, toxicity and handling characteristics.

Table 1. Description of reagents used for the synthesis

Reagent	Formula	Purity	Toxicity	Handling
Sodium tungstate dihydrate	$Na_2WO_4 \cdot 2H_2O$	99.0 - 101.0 %	Harmful	Fume hood and rubber gloves
Hydrochloric acid	HCl	37 %	Corrosive and irritant	Fume hood and rubber gloves
Phosphoric acid	H_3PO_4	85 %	Corrosive	Fume hood and rubber gloves
Potassium chloride	KCl	100.1 %	None	Rubber gloves
Tetrabutylammonium bromide	$[Bu_4N]Br$	≥ 99.0 %	Corrosive	Fume hood and rubber gloves
Potassium hydrogen carbonate	$KHCO_3$	> 99.0 %	None	Rubber gloves
Sulfuric acid	H_2SO_4	> 95 %	Corrosive	Fume hood and rubber gloves
Phosphonic acid	H_3PO_3	≥ 98.5 %	Corrosive	Fume hood and rubber gloves
Nickel chloride dihydrate	$NiCl_2 \cdot 2H_2O$	99.95 %	Harmful, toxic and carcinogenic	Fume hood and rubber gloves

In the following **Table 2**, solvents used in this project are named as well as their purity, toxicity and handling characteristics.

Table 2. Description of solvents used for the synthesis

Solvent	Formula	Purity	Toxicity	Handling
N,N-dimethylformamide	C_3H_7NO	> 99 %	Flammable, irritant and carcinogenic	Fume hood and rubber gloves
Dichloromethane	CH_2Cl_2	99.99 %	Irritant and carcinogenic	Fume hood and rubber gloves
Diethyl ether	$(C_2H_5)_2O$	≥ 99 %	Flammable and irritant	Fume hood and rubber gloves
Acetonitrile	C_2H_3N	99.99 %	Flammable and irritant	Fume hood and rubber gloves
N,N-dimethylacetamide	C_4H_9NO	99 %	Irritant, carcinogenic and harmful	Fume hood and rubber gloves

4.2. Instruments

Several techniques have been used to characterise all products and to investigate the chemical properties that polyoxometalates show. Elemental analysis, nuclear magnetic resonance, cyclic voltammetry, infrared spectroscopy and ultraviolet-visible spectroscopy are the techniques that have been used throughout the project, each one of which provides different information about POMs and their hybrids.

In this project, the data for elemental analysis has been obtained from a CE-440 Elemental Analyser manufactured by Exeter Analytical. Proton (^{1}H NMR) and phosphorous (^{31}P NMR) nuclear magnetic resonance were obtained using a Bruker DPX 300 spectrometer. To collect ^{1}H NMR data a 16 scans mode was used and for ^{31}P NMR, a 128 scans proton decoupled mode was used. Infrared spectra were measured using a Bruker Alpha FTIR spectrometer with a platinum ATR module. Cyclic voltammograms were measured in an Electrochemical Analyzer by CH Instruments, with a glassy carbon working electrode. The formal reference electrode was a silver wire although Fc/Fc^+ (ferrocene) was used as an external reference. The counter electrode was a platinum wire. The samples were measured in dry N,N-dimethylformamide as the solvent and tetrabutylammonium hexafluorophosphate ($TBAPF_6$) as the supporting electrolyte. Ultraviolet-visible spectroscopy data was recorded using a Lambda 25 Perkin Elmer spectrometer.

4.3. Synthesis

4.3.1. Synthesis of $K_6[P_2W_{18}O_{62}] \cdot 14H_2O$

$$18\ Na_2WO_4 \cdot 2H_2O + 32\ H_3PO_4 + 6KCl \longrightarrow \mathbf{K_6[P_2W_{18}O_{62}] \cdot 14H_2O} + 30\ Na[H_2PO_4] + 40\ H_2O + 6\ NaCl \quad \textbf{(2)}$$

Following Finke *et al.* procedure[30], 10 g of $Na_2WO_4 \cdot 2H_2O$ (30.3 mmol) was dissolved in 12 mL of deionised water in a 50 mL round-bottom flask with vigorous stirring. After the complete dissolution, a colourless solution was obtained, 8.35 mL of 4 M HCl (33.3 mmol) was added *via* a dropping funnel (2 drops/s) with stirring. The solution is left for 10 additional minutes so that the milky white precipitate produced redissolves. After that, the resulting pH is between 6 and 7. Next, 8.35 mL of H_3PO_4 (33.3 mmol) was added with a dropping funnel (4 drops/s) and this provoked the formation of a milky solid which redissolves to give a pale yellow clear solution with pH between 1 and 2. The solution was heated up to 115 ˚C and refluxed for 24 hours. Afterwards, the solution was cooled to room temperature and 5 g of KCl (67 mmol) was added with stirring. After 10 minutes, a chalky yellow precipitate had been formed. The solid was then filtered and dried on the frit by aspiration for 1 hour. To recrystallize, the crude material was transferred into a 50 mL beaker and dissolved, with stirring, in 22 mL of water at 80 ˚C. The solution was evaporated until the volume was less than 5 mL and next, it was left cooling in the fridge. After 72 hours, yellow crystals had been formed. Once dried, 6.991 g of $K_6[P_2W_{18}O_{62}] \cdot 14H_2O$ (**Eq. 2**) was obtained. Yield: 86 %.

Characterisation – ^{31}P NMR [δ, D_2O]: -12.76 ppm. IR (ATR) cm^{-1}: 1085 [P-O stretch], 952 [$W{=}O_d$ stretch], 901 [$W\text{-}O_b\text{-}W$ stretch] and 726 [$W\text{-}O_c\text{-}W$ stretch].

4.3.2. Synthesis of $[Bu_4N]_6[P_2W_{18}O_{62}]$

$$K_6[P_2W_{18}O_{62}] \cdot 14H_2O + 6\ [Bu_4N]Br \longrightarrow \mathbf{[Bu_4N]_6[P_2W_{18}O_{62}]} + 6\ KBr + 14\ H_2O \quad \textbf{(3)}$$

As previously done in the group, 1.9 g of $K_6[P_2W_{18}O_{62}] \cdot 14H_2O$ (0.392 mmol) was dissolved in 90 mL of deionised water resulting in a transparent yellow solution. Next, 1.25 g of $[Bu_4N]Br$ (3.88 mmol) was dissolved in 10 mL of water. The $[Bu_4N]Br$ solution was added dropwise into the $K_6[P_2W_{18}O_{62}]$ solution. The immediate formation of a milky

white precipitate was observed and the mixture was left stirring for 1 hour. The solvent was evaporated *via* heating giving a white solid. After that, the product was gently washed with water and then filtered by aspiration on a frit. After drying the product under vacuum, 2.146 g of a yellowish white solid was obtained as $[Bu_4N]_6[P_2W_{18}O_{62}]$ (**Eq. 3**). Yield: 94 %.

Characterisation – ^{31}P NMR [δ, DMSO-d_6]: -13.22 ppm. ^{1}H NMR [δ, DMSO-d_6]: triplet (12H, CH_3-), sextet (8H, -CH_2-), quintet (8H, -CH_2-) and triplet (8H, -CH_2-N^+). IR (ATR) cm^{-1}: 2961 [CH stretch], 1484 [CH_2 wagging], 1379 [CH_3 wagging], 1088 [P-O stretch], 952 [W=O_d stretch], 903 [W-O_b-W stretch] and 769 [W-O_c-W stretch].

4.3.3. Synthesis of $K_{10}[P_2W_{17}O_{61}] \cdot 15H_2O$

$$7\ K_6[P_2W_{18}O_{62}] \cdot 14H_2O + 34\ KHCO_3 \longrightarrow 7\ \mathbf{K_{10}[P_2W_{17}O_{61}] \cdot 15H_2O} + K_6[W_7O_{24}] + 34\ CO_2 + 10\ H_2O \quad \textbf{(4)}$$

Following Finke *et al.* procedure[31], a solution of 2 g of $K_6[P_2W_{18}O_{62}] \cdot 14H_2O$ (0.412 mmol) in 5 mL of deionised water and a solution of 0.54 g of $KHCO_3$ (5.39 mmol) in 5 mL of deionised water were prepared. The $KHCO_3$ solution was added dropwise into the $K_6[P_2W_{18}O_{62}]$ with stirring. After 1 hour, the reaction was complete and a white precipitate had formed. The precipitate was then filtered off and dried under suction with a glass frit. The crude white solid was recrystallized by dissolving it in 16 mL of hot water at 120 ˚C. Once dissolved, the solution was hot filtrated to remove any insoluble impurities and was left to cool to room temperature. The solution was then left to cool in the fridge. After filtering the white precipitate and drying it, 1.415 g of $K_{10}[P_2W_{17}O_{61}] \cdot 15H_2O$ was obtained (**Eq. 4**). Yield: 71 %.

Characterisation – ^{31}P NMR [δ, D_2O]: -6.96 and -14.12 ppm. IR (ATR) cm^{-1}: 1079 [P-O stretch], 1049 [P-O stretch], 1014 [P-O stretch], 936 [W=O_d stretch], 882 [W=O_d stretch], 798 [W-O_b-W stretch] and 716 [W-O_c-W stretch].

4.3.4. Synthesis of $[Bu_4N]_8H_2[P_2W_{17}O_{61}]$

$$K_{10}[P_2W_{17}O_{61}] \cdot 15H_2O + 8\ [Bu_4N]Br \longrightarrow \mathbf{[Bu_4N]_8H_2[P_2W_{17}O_{61}]} + 8\ KBr + 2\ KOH + 13\ H_2O \quad \textbf{(5)}$$

Following Francesconi *et al.* procedure[32], 1 g of $K_{10}[P_2W_{17}O_{61}] \cdot 15H_2O$ (0.220 mmol) was dissolved in 100 mL of deionised water resulting in a clear solution, pH 6.2. The pH was gradually adjusted to 5.65 by adding 0.18 M H_2SO_4. Then, 0.567 g of $[Bu_4N]Br$ (1.76 mmol) was slowly added while the pH of the solution was maintained in the range of 5.5 and 7.5 with 0.18 M H_2SO_4. The resulting white cloudy solution was then extracted with 6.8 mL of acetonitrile and 13.4 mL of dichloromethane. After extracting the mixture for 5 minutes, the clear organic layer was collected and solvent removed under reduced pressure. Next, the solid was dissolved in 1 mL of dichloromethane resulting in a green-yellow solution and the addition of 5 mL of diethyl ether caused the precipitation of a white solid. The precipitate was filtered off and dried under vacuum. No further recrystallization from acetonitrile was required. Finally, 456 mg of $[Bu_4N]_8H_2[P_2W_{17}O_{61}]$ was obtained as a white powder (**Eq. 5**). Yield: 36 %.

Characterisation – ^{31}P NMR [δ, DMSO-d_6]: -9.3 and -13.61 ppm. ^{1}H NMR [δ, DMSO-d_6]: triplet (12H, CH_3-), sextet (8H, -CH_2-), quintet (8H, -CH_2-) and triplet (8H, -CH_2-N^+). IR (ATR) cm^{-1}: 2959 [CH stretch], 1484 [CH_2 wagging], 1379 [CH_3 wagging], 1081 [P-O stretch], 1055 [P-O stretch], 1030 [P-O stretch], 938 [W=O_d stretch], 915 [W=O_d stretch], 882 [W-O_b-W stretch] and 772 [W-O_c-W stretch].

4.3.5. Synthesis of $[Bu_4N]_5K[P_2W_{17}O_{57}(HPO_3)_2]$

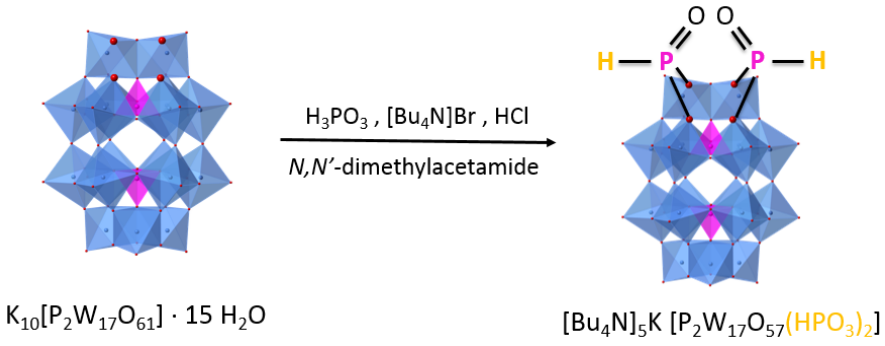

Figure 11. Equation for the synthesis of $[Bu_4N]_5K[P_2W_{17}O_{57}(HPO_3)_2]$.

As previously done in the group[c], 1 g of $K_{10}[P_2W_{17}O_{61}] \cdot 15H_2O$ (0.203 mmol) was added to a 50 mL round-bottom flask. Next, 656 mg of $[Bu_4N]Br$ (2.03 mmol) and 33.4 mg of H_3PO_3 (0.406 mmol) was also added. 30 mL of N,N-dimethylacetamide was used as the solvent and finally, 100 µL of 12 M HCl was also added resulting in a yellow milky

[c] Manuscript in preparation. Not published yet.

solution. The solution was then refluxed at 80 ˚C for 24 hours. In order to avoid the photoreduction of the hybrid, the flask was covered with aluminium foil. As the reaction progressed the mixture turned into a transparent yellow solution. Once complete, the mixture was filtered in order to remove any insoluble impurities and non-reacted substances. The solution was then distributed among 4 centrifuge tubes and they were filled with diethyl ether. Upon agitation, a white milky suspension was formed. The tubes were centrifuged at 5000 rpm for 5 minutes. A yellow oil appeared at the bottom of the tubes and the clear solvent was removed. Next, 5 mL of acetonitrile was added into each of the tubes and following the sonication process to make homogeneous mixtures, diethyl ether was again added to fill up the tubes and precipitate the hybrid. The tubes were centrifuged again and the acetonitrile addition was carried out one more time to obtain a white solid at the bottom of the tubes – though sometimes the solid was blue greenish due to reduction. The clear solvent was eventually removed and the tubes were left open to fully dry the product. 950 mg of a blueish white powder was obtained as $[Bu_4N]_5K[P_2W_{17}O_{57}(HPO_3)_2]$ (**Fig. 11**). Yield: 85 %.

Characterisation – ^{31}P NMR [δ, DMSO-*d*$_6$]: 4.25, -11.03 and -12.65 ppm. ^{1}H NMR [δ, DMSO-*d*$_6$]: triplet (12H, CH_3-), sextet (8H, -CH_2-), quintet (8H, -CH_2-) and triplet (8H, -CH_2-N^+). IR (ATR) cm^{-1}: 2961 [CH stretch], 1481 [CH_2 wagging], 1379 [CH_3 wagging], 1155 [P-O stretch], 1110 [P-O stretch], 1085 [P-O stretch], 1053 [P-O stretch], 1024 [P-O stretch], 954 [W=O_d stretch], 907 [W=O_d stretch], 888 [W-O_b-W stretch] and 733 [W-O_c-W stretch].

4.3.6. Synthesis of $[Bu_4N]_5K[P_2W_{17}O_{57}(HPO_4)_2]$

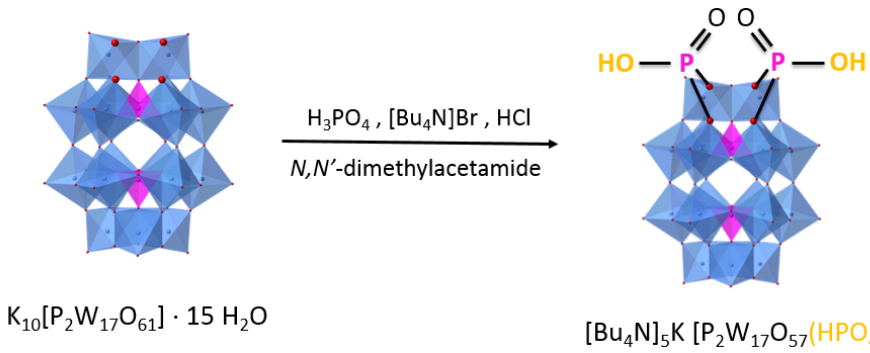

Figure 12. Equation for the synthesis of $[Bu_4N]_5K[P_2W_{17}O_{57}(HPO_4)_2]$.

As previously done in the group[d], 1 g of $K_{10}[P_2W_{17}O_{61}] \cdot 15H_2O$ (0.203 mmol) was added to a 50 mL round-bottom flask. Next, 656 mg of $[Bu_4N]Br$ (2.03 mmol) and 27.6 µL of 85 % H_3PO_4 (0.406 mmol) was also added. 30 mL of N,N-dimethylacetamide was used as the solvent and finally, 100 µL of 12 M HCl was also added resulting in a yellow milky solution. The solution was then refluxed at 60 ˚C for 24 hours. In order to avoid the photoreduction of the hybrid, the flask was covered with aluminium foil. As the reaction progressed the mixture turned into a transparent yellow solution. Once complete, the mixture was filtered in order to remove any insoluble impurities and non-reacted substances. The solution was then distributed among 4 centrifuge tubes and they were filled with diethyl ether. Upon agitation, a white milky suspension was formed. The tubes were centrifuged at 5000 rpm for 5 minutes. A yellow oil appeared at the bottom of the tubes and the clear solvent was removed. Next, 5 mL of acetonitrile was added into each of the tubes and following the sonication process to make homogeneous mixtures, diethyl ether was again added to fill up the tubes and precipitate the hybrid. The tubes were centrifuged again and the acetonitrile addition was carried out one more time to obtain a white solid at the bottom of the tubes – though sometimes the solid was blue greenish due to reduction. The clear solvent was eventually removed and the tubes were left open to fully dry the product. 986 mg of a white powder was obtained as $[Bu_4N]_5K[P_2W_{17}O_{57}(HPO_4)_2]$ (**Fig. 12**). Yield: 87 %.

Characterisation – ^{31}P NMR [δ, DMSO-d_6]: -4.29, -10.98 and -12.86 ppm. ^{1}H NMR [δ, DMSO-d_6]: triplet (12H, CH_3-), sextet (8H, -CH_2-), quintet (8H, -CH_2-) and triplet (8H, -CH_2-N^+). IR (ATR) cm^{-1}: 2959 [CH stretch], 1484 [CH_2 wagging], 1379 [CH_3 wagging], 1085 [P-O stretch], 1053 [P-O stretch], 999 [P-O stretch], 954 [W=O_d stretch], 907 [W=O_d stretch], 813 [W-O_b-W stretch] and 733 [W-O_c-W stretch].

In this case, the further purification of the product is difficult mainly due to the remaining presence of H_3PO_4 starting material impurities. Washing with different solvents was attempted, such as acetonitrile, ethanol, water or acetone, but unfortunately the impurity could not be removed. This fact made us suspect that the H_3PO_4 was in some way incorporated into the hybrid polyoxotungstate structure thanks to hydrogen bonds (**Fig. 13**). Further study needs to be done in this issue.

[d] Manuscript in preparation. Not published yet.

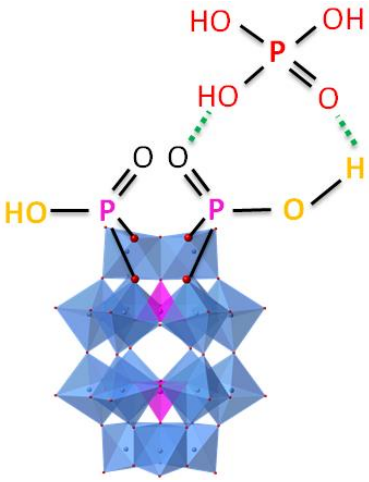

Figure 13. Hydrogen-bond interactions established between the phosphonate hybrid polyoxotungstate and the phosphoric acid that might hinder proper purification of the product.

4.3.7. Attempts of organofunctionalisation

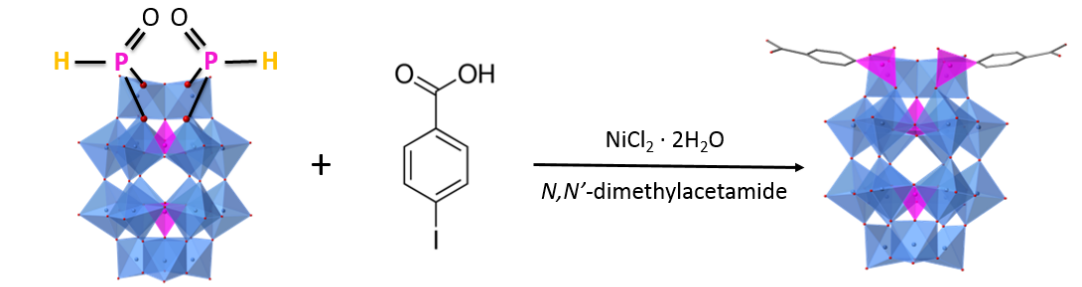

$[Bu_4N]_5K\,[P_2W_{17}O_{57}(HPO_3)_2]$ 4-iodobenzoic acid $[Bu_4N]_5K[P_2W_{17}O_{57}(PO_5H_5C_7)_2]$

Figure 14. Addition of 4-iodobenzoic acid to $[Bu_4N]_5K[P_2W_{17}O_{57}(HPO_3)_2]$.

The addition of 4-iodobenzoic acid (**Fig. 14**) in several conditions, such as time, temperature and light, has been performed with the phosphonate hybrid, $[Bu_4N]_5K[P_2W_{17}O_{57}(HPO_3)_2]$. The catalyst used was $NiCl_2 \cdot 2H_2O$ and the solvent, *N,N*-dimethylacetamide (DMA). **Table 3** summarises different attempted experiences.

Table 3. Conditions of time, temperature and light for each experiment.

Experience	Time	Temperature	Microwave	Final
1	24 h	90 ˚C	No	Non hydrolised
2	2 h	90 ˚C	Yes	Non hydrolised
3	4 h	90 ˚C	Yes	Non hydrolised
4	96 h	130 ˚C	No	Non hydrolised
5	2 h	130 ˚C	Yes	Hydrolised
6	4 h	130 ˚C	Yes	Hydrolised

Nevertheless, none of the experiences were successful. What can be concluded from them is that hybrid starting material is that temperature favours the hydrolysis. In experience 5, the hybrid was beginning to hydrolyse whereas in experience 6, it was completely hydrolysed. This fact also means that the longer the reaction is run, the higher the decomposition of the hybrid. Finally, visible light may avoid the hydrolysis though more experiences at higher temperature are needed.

5. Results and discussion

In this section, results regarding the characterisation of the compounds will be shown and discussed. Another aim of this section is to compare how data varies depending on the chemical structure of the polyoxometalate, from heteropolyoxometalates, going over to lacunary POMs to phosphate and phosphonate hybrids.

5.1. CHN elemental analysis

CHN elemental analysis involves a process where a sample is analysed for its elemental composition. Carbon, hydrogen and nitrogen content are determined by combustion analysis; a sample is burned in an excess of oxygen and various traps collect the combustion products: carbon dioxide, water, and nitric oxide. The masses of these combustion products are used to calculate the composition of the sample.

For polyoxometalates, which do not contain any carbon, hydrogen or nitrogen elements in its structure, elemental analysis is useful to check the purity of the product as well as to show whether the product is dry or still contains solvent and also to see if any water molecules are coordinated to the compound.

This process becomes more informative if polyoxometalates contain any of the stated elements. This is relevant for POM-based hybrids and also for all polyoxometalates with organic counter ions. In all of these cases, by using the weight percentages obtained for carbon, hydrogen and nitrogen, a chemical formula is calculated to fit those results. Thus, precise molecular weight can be obtained.

Each synthesised product was characterised and purity tested with CHN microanalysis. **Table 4** below summarises the results.

Table 4. CHN microanalysis for all the synthesised compounds showing the predicted and experimental weight percentage for carbon, hydrogen and nitrogen elements. Values which are within the 0.3% error are coloured green whereas those outside of this margin are coloured red.

		% C	% H	% N
$K_6[P_2W_{18}O_{62}] \cdot 14H_2O$	Experimental	0	0.24	0
	Predicted	0	0.58	0
$[Bu_4N]_6[P_2W_{18}O_{62}]$	Experimental	20.96	3.97	1.46
	Predicted	19.82	3.74	1.44
$K_{10}[P_2W_{17}O_{61}] \cdot 15H_2O$	Experimental	0	0.48	0
	Predicted	0	0.82	0
$[Bu_4N]_8H_2[P_2W_{17}O_{61}]$	Experimental	25.39	4.78	1.91
	Predicted	25.18	4.79	1.84
$[Bu_4N]_5K[P_2W_{17}O_{57}(HPO_3)_2]$	Experimental	17.55	3.34	1.17
	Predicted	17.44	3.33	1.27
$[Bu_4N]_5K[P_2W_{17}O_{57}(HPO_4)_2]$	Experimental	16.74	3.12	1.08
	Predicted	17.34	3.31	1.26

From the data above it is clear that the target materials were all successfully obtained as most of the experimental weight percentages are relatively close to the predicted ones. Nevertheless, the fact that there are small errors and deviations from the predicted values suggests that there are some impurities, either because of remaining solvent molecules or non-desired derivatives.

Regarding $K_6[P_2W_{18}O_{62}] \cdot 14H_2O$ and $K_{10}[P_2W_{17}O_{61}] \cdot 15H_2O$ polyoxotungstates, it needs to be taken into consideration that when some of the elements analysed are not present – carbon and nitrogen in these cases – or those that are present are in very little amounts, it may be possible that the results vary from the real ones. However, in both cases the difference in the values implies a lower number of coordinated water molecules than those reported in the synthetic procedures as the experimental hydrogen content is

always lower than the predicted value. This is due to the fact that water content in polyoxometalates is variable and differs based on the rigorousness of drying used.

Regarding $[Bu_4N]_6[P_2W_{18}O_{62}]$, the difference in the carbon content may probably mean the presence of remaining solvent molecules such as acetone, or impurities such as grease.

5.2. Nuclear magnetic resonance spectrometry

Nuclear magnetic resonance (NMR) is a technique commonly used to quickly characterise polyoxometalates. In this work, phosphorous resonance (^{31}P NMR) was employed to see whether the product had been successfully obtained and also to check its purity.

Thanks to the different symmetries and surroundings of phosphorous atoms in POMs synthesised in the project, one two or up to three peaks were seen in the spectra and this allows a fast identification of the Wells-Dawson heteropolyoxotungstate, the lacunary analogue and the inorganic hybrids as well.

When organic counter ions are involved and for future organofunctionalisation work as well, proton resonance (^1H NMR) is also convenient for the characterisation of the product and to monitor the reaction and verify if the addition has occurred. Regarding carbon resonance (^{13}C NMR), this is also useful for organic characterisation though it needs to be taken into consideration the large amount of sample required per measurement.

In $[P_2W_{18}O_{62}]^{6-}$ salts, one single sharp peak is observed because of the symmetry of the structure that makes both phosphorous atoms equivalent, although the shifts may differ depending on the counter ions. Meanwhile, in the lacunary analogue, $[P_2W_{17}O_{61}]^{10-}$ salts, phosphorous atoms are no longer environmentally equal and this is shown in the NMR spectra as two different peaks. Upon the addition of phosphate and phosphonate groups, a third peak appears due to the new phosphorous atoms attached, which are equivalent to each other (**Fig. 15**).

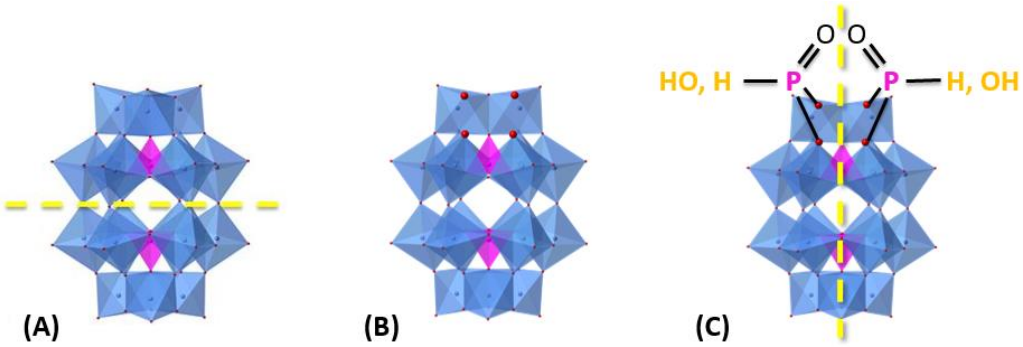

Figure 15. Simmetry in different POM structures: (A) $[P_2W_{18}O_{62}]^{6-}$ salts, 1 single peak in ^{31}P NMR / (B) $[P_2W_{17}O_{61}]^{10-}$ salts, 2 peaks in ^{31}P NMR / (C) Inorganic hybrids, 3 peaks in ^{31}P NMR

Potassium salts spectra were recorded in deuterium oxide (D_2O) whereas the tetrabutylammonium organic salts were recorded in deuterated dimethylsulfoxide (DMSO-d_6) because of solubility differences.

In **Fig. 16**, potassium and tetrabutylammonium salts ^{31}P NMR spectra for Wells-Dawson polyoxotungstates are showed. In both cases, two small peaks appear up field of the product. They mean that the product is not isomerically pure.

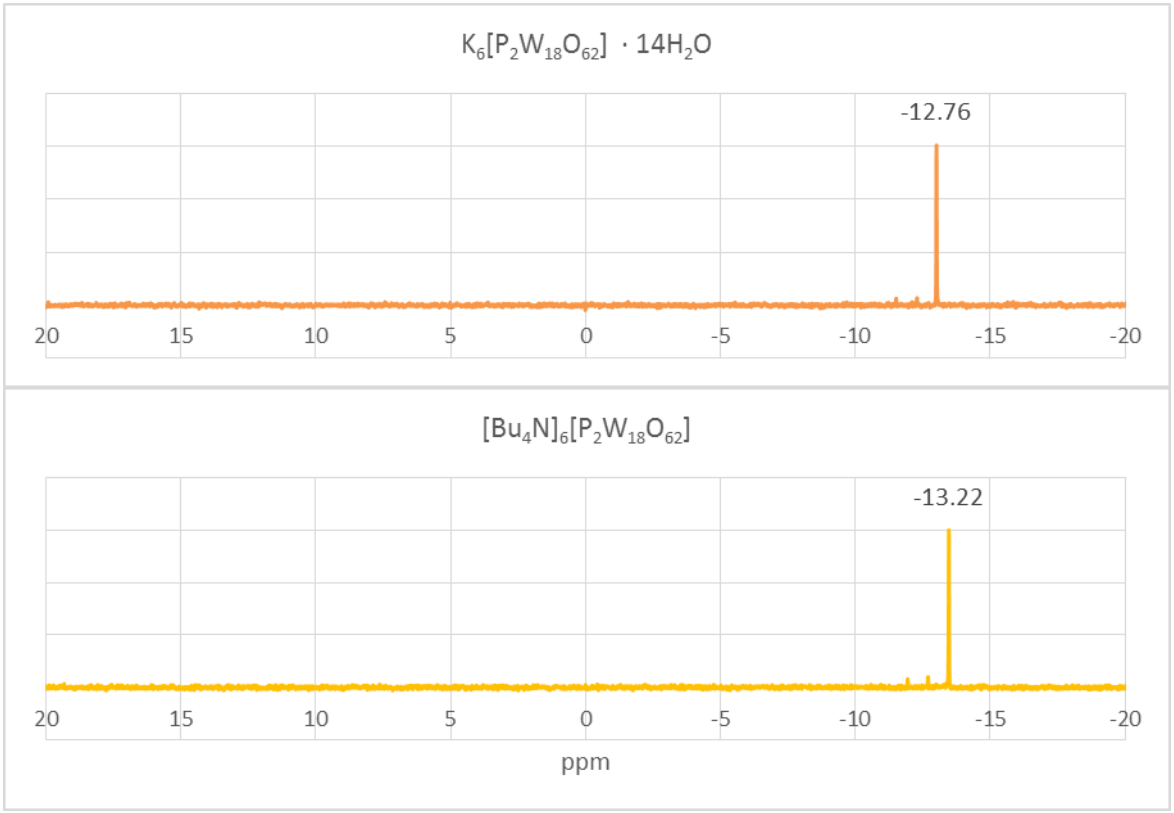

Figure 16. ^{31}P NMR for $K_6[P_2W_{18}O_{62}] \cdot 14H_2O$ and $[Bu_4N]_6[P_2W_{18}O_{62}]$ respectively.

In **Fig. 17**, ^{1}H NMR spectra for the tetrabutylammonium salt of the Wells-Dawson polyoxotungstate is showed, with assignments based on chemical shift and multiplicity.

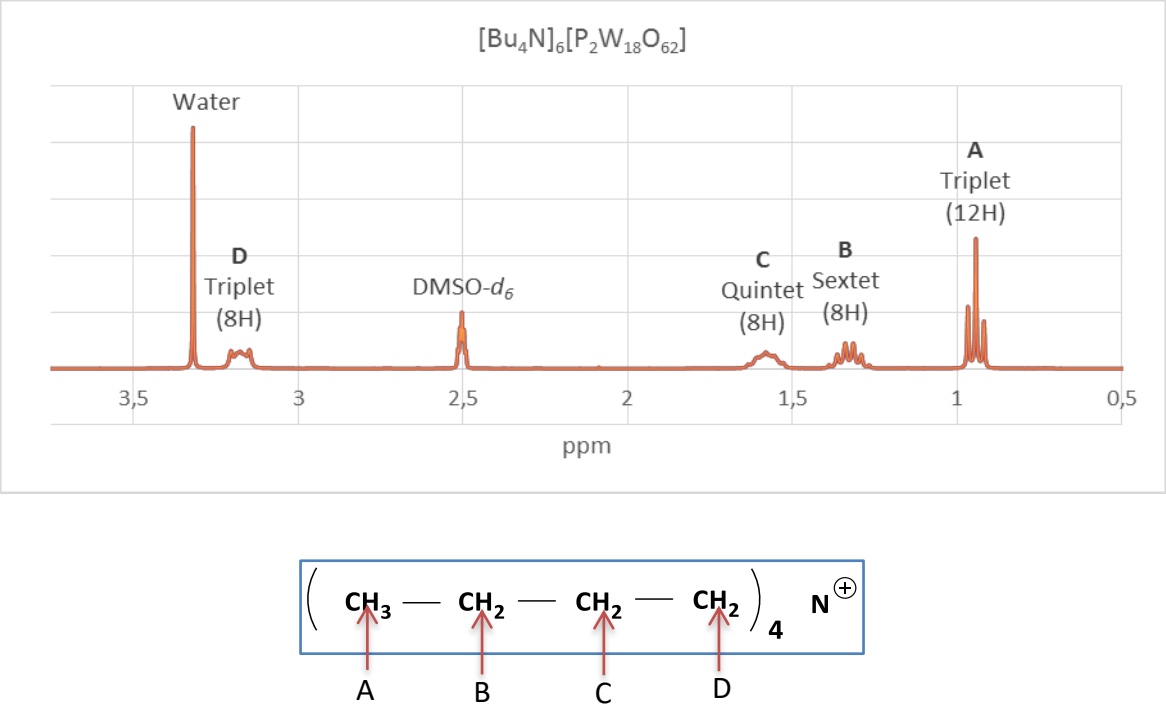

Figure 17. ^{1}H NMR for $[Bu_4N]_6[P_2W_{18}O_{62}]$.

In **Fig. 18**, potassium and tetrabutylammonium salts ^{31}P NMR spectra for lacunary Wells-Dawson polyoxotungstates are showed. ^{1}H NMR showing the organic counter ion is very similar to **Fig. 17**. As can clearly be seen, the lacuna introduces asymmetry into the phosphorous environments of the POM resulting in the phosphorous atom closest to the lacuna being upshifted to -6.96 ppm.

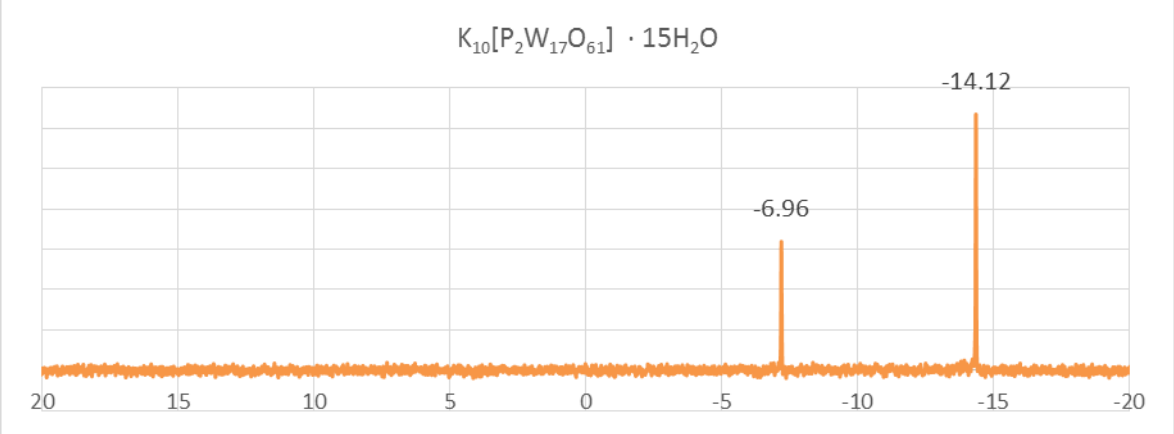

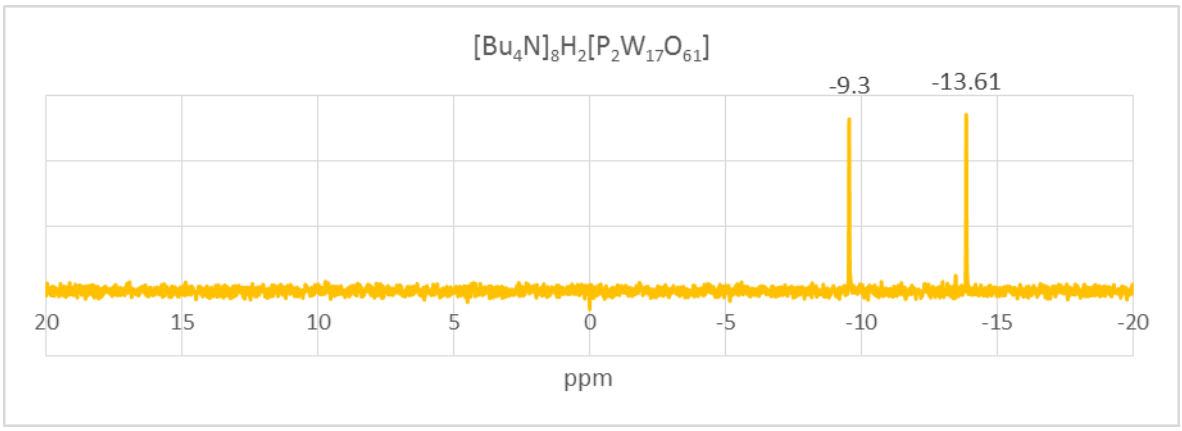

Figure 18. ^{31}P NMR for $K_{10}[P_2W_{17}O_{61}] \cdot 15H_2O$ and $[Bu_4N]_8H_2[P_2W_{17}O_{61}]$respectively.

Regarding the synthesis of the inorganic hybrids, **Fig. 19** shows the ^{31}P NMR for all the tetrabutylammonium salts. As previously said, the lacuna introduces asymmetry and this results in an additional second peak at -9.3 ppm. Moreover, in the hybrids structures, two more phosphorous atoms are introduced into the structure, from the phosphonate and phosphate groups, and as they are both equivalent, only a new third peak appears at 4.25 and -4.29 respectively.

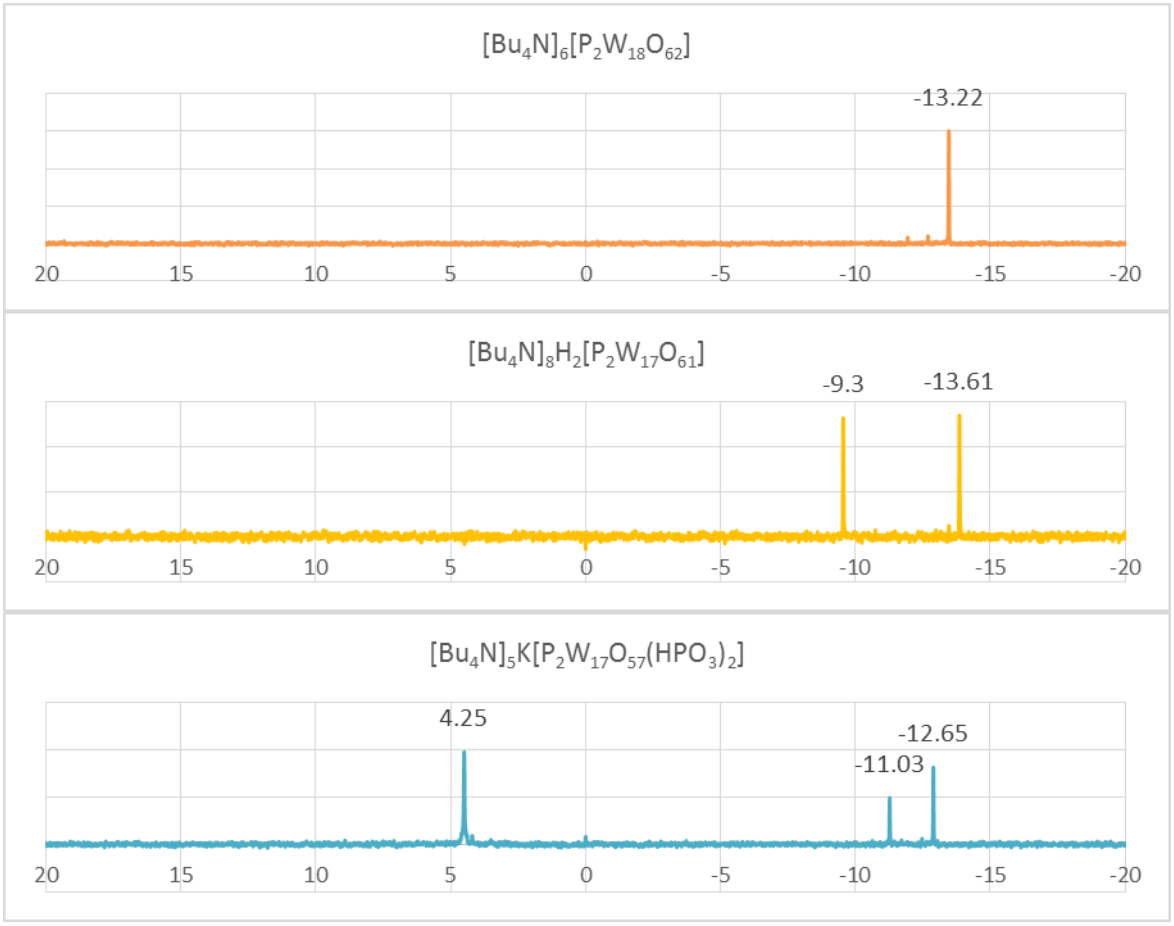

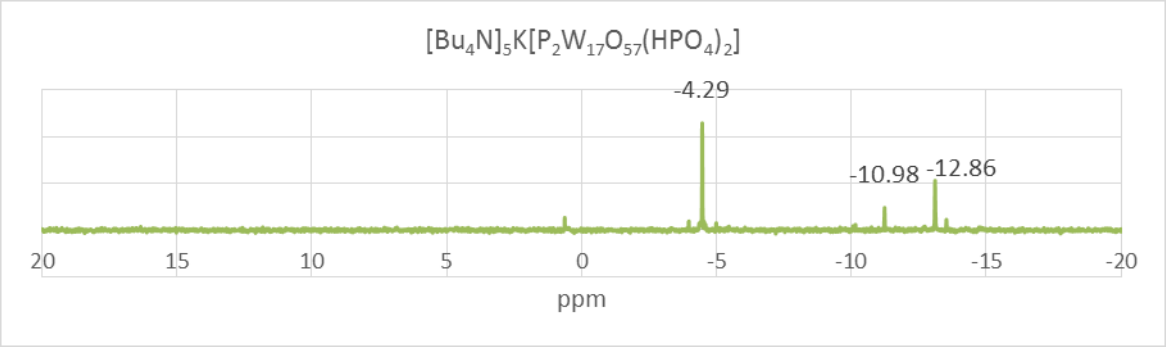

Figure 19. ^{31}P NMR for $[Bu_4N]_6[P_2W_{18}O_{62}]$, $[Bu_4N]_8H_2[P_2W_{17}O_{61}]$, $[Bu_4N]_5K[P_2W_{17}O_{57}(HPO_3)_2]$ and $[Bu_4N]_5K[P_2W_{17}O_{57}(HPO_4)_2]$ respectively.

5.3. Infrared spectroscopy

Attenuated total reflectance (ATR) infrared spectroscopy is commonly used to identify substances. This technique exploits the fact that molecules absorb infrared radiation causing the vibration of bonds that are characteristic of their structure. It is especially useful to check if the hybridisation has been successful as the hybrid spectra is supposed to be made of bands from the inorganic POM cluster as well as the free organic ligand.

Regarding following data, a nomenclature is used to distinguish among different types of oxygen. O_d is the double-bonded oxygen linked to a tungsten, O_b is the bridging oxygen located between a couple of tungsten atoms and finally, O_c is the oxygen which is contained in the phosphorous atom coordination tetrahedral.

In following images (**Fig. 20-25**), all the infrared data will be showed regarding all the products.

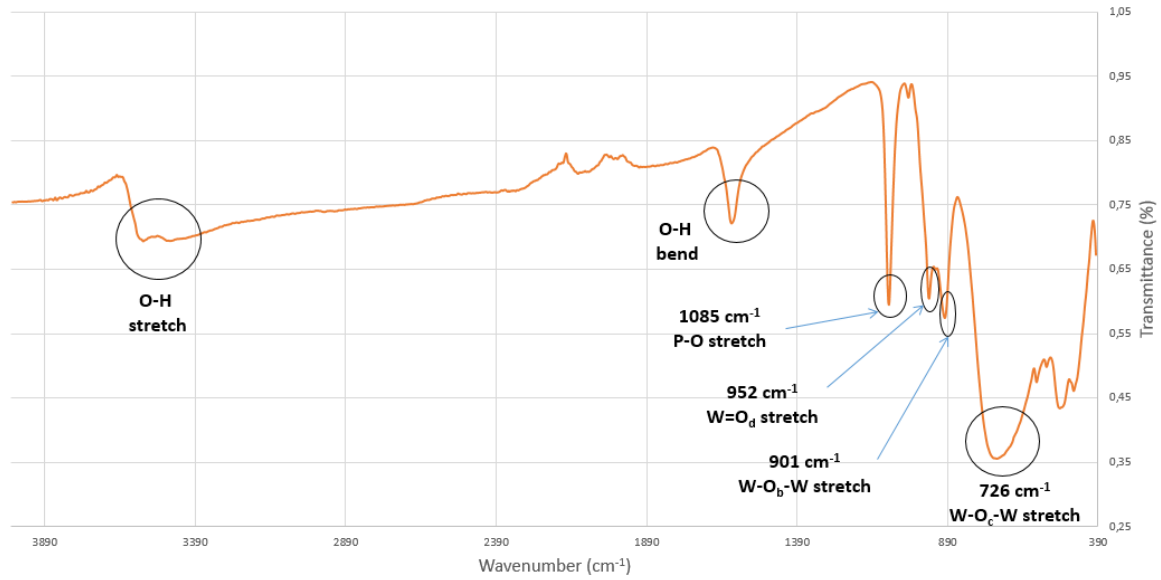

Figure 20. IR data for $K_6[P_2W_{18}O_{62}] \cdot 14\ H_2O$

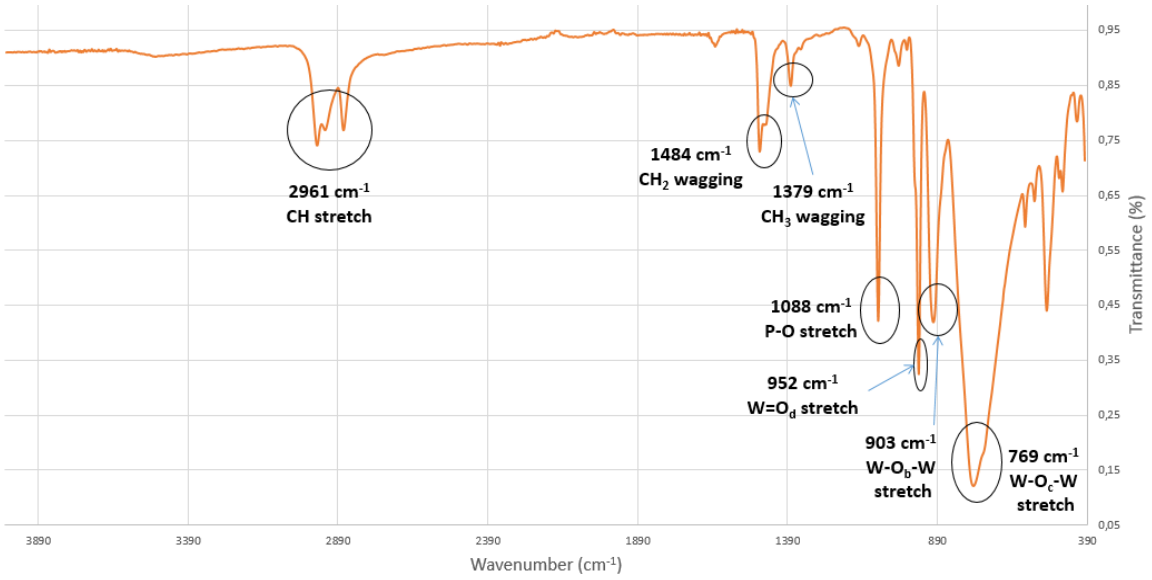

Figure 21. IR data for $[Bu_4N]_6[P_2W_{18}O_{62}]$

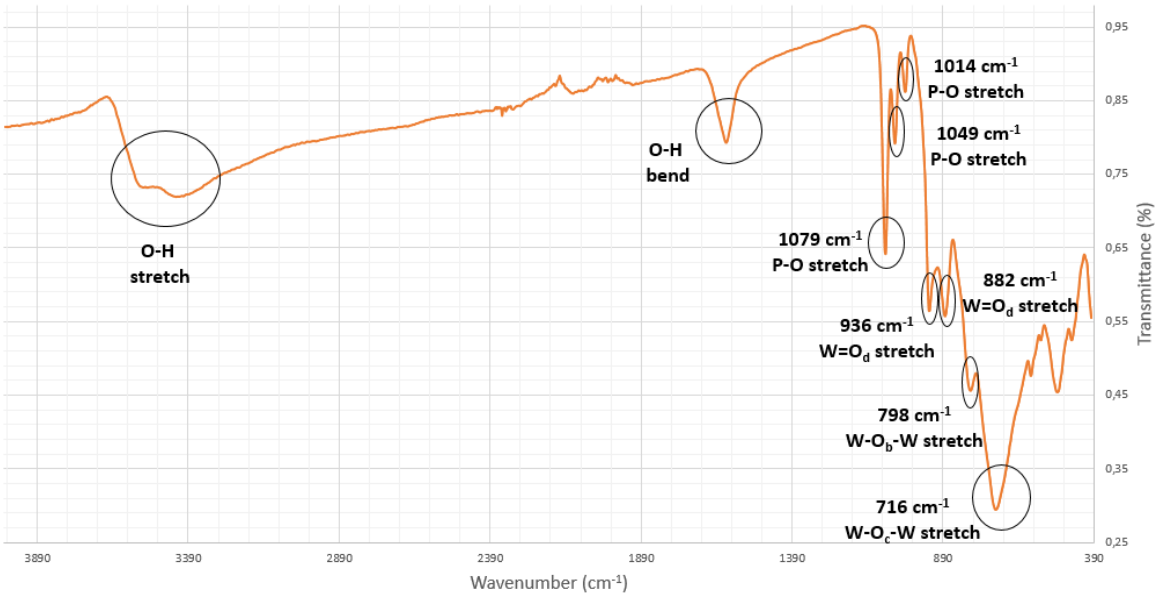

Figure 22. IR data for $K_{10}[P_2W_{17}O_{61}] \cdot 15H_2O$

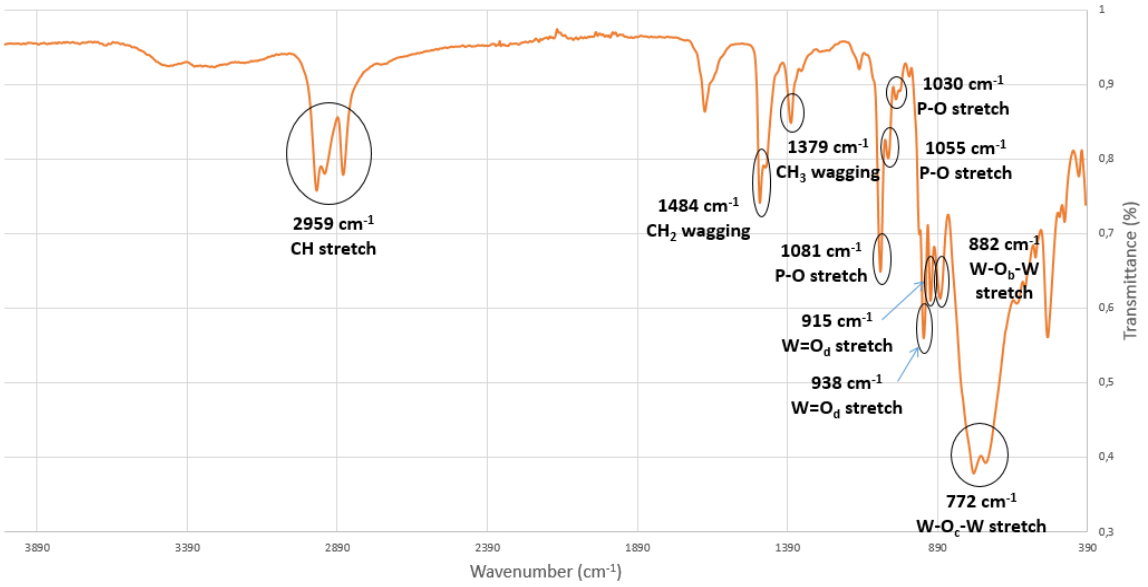

Figure 23. IR data for $[Bu_4N]_8H_2[P_2W_{17}O_{61}]$

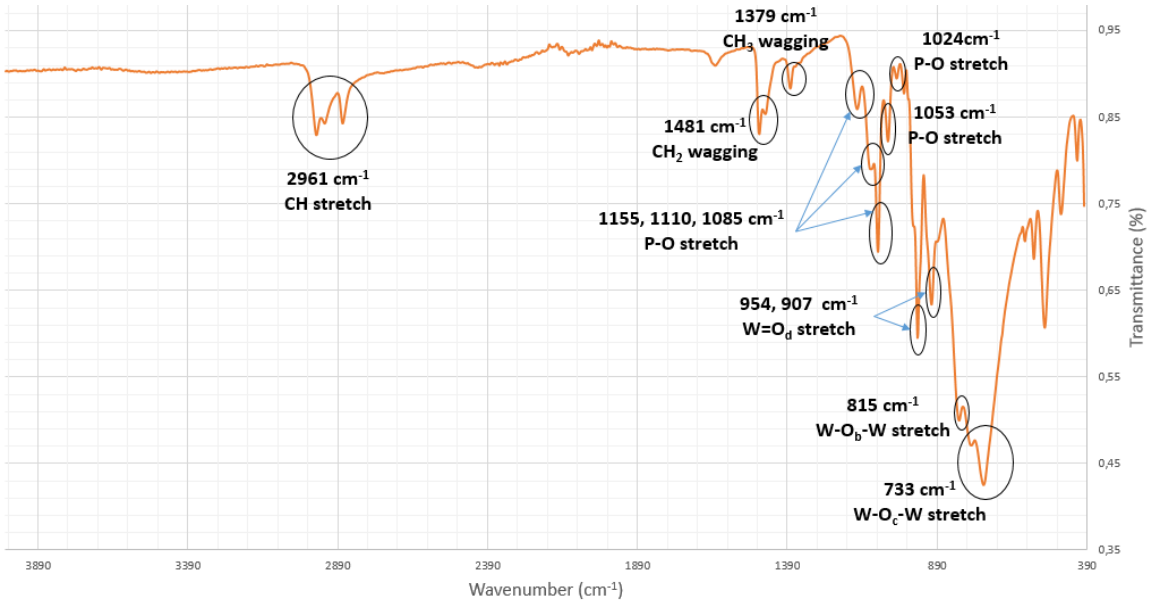

Figure 24. IR data for $[Bu_4N]_5K[P_2W_{17}O_{57}(HPO_3)_2]$

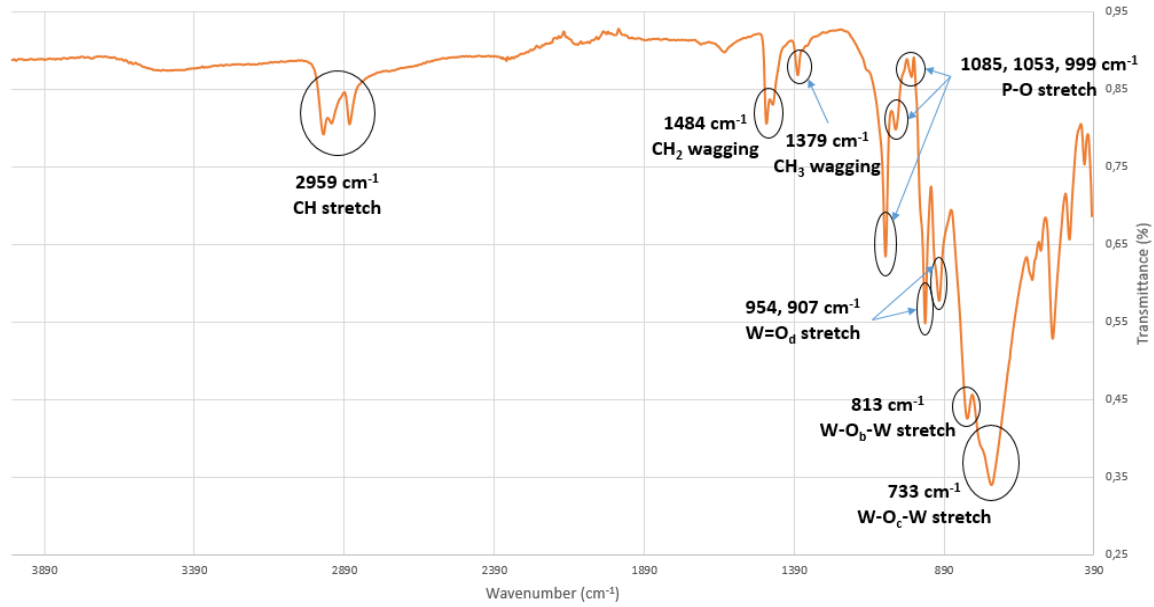

Figure 25. IR data for $[Bu_4N]_5K[P_2W_{17}O_{57}(HPO_4)_2]$

Several peaks have been identified in the spectra. Broad bands appear for the O-H bend when water molecules are coordinated to the potassium salts. When the counter ion is tetrabutylammonium, new peaks appear for the carbon-hydrogen stretching and wagging. Phosphorous-oxygen stretching bands appear all in the range of 1150-1000 cm^{-1} whereas those bonds involving tungsten atoms appear in the range of 910-700 cm^{-1}.

5.4. Cyclic voltammetry

Cyclic voltammetry (CV) is an electrochemical measurement used to study the redox properties of an analyte in solution. In these type of experiments, the carbon working electrode potential is ramped linearly versus time. After the set potential is reached, the potential is ramped in the opposite direction to return to the initial potential.

In the initial ramp towards negative potentials, the polyoxometalate is being reduced and each peak corresponds to one or more electrons being incorporated into the POM's structure. In the ramp towards positive potential, the opposite phenomenon occurs and the POM is oxidised back to its initial state (**Fig. 26**).

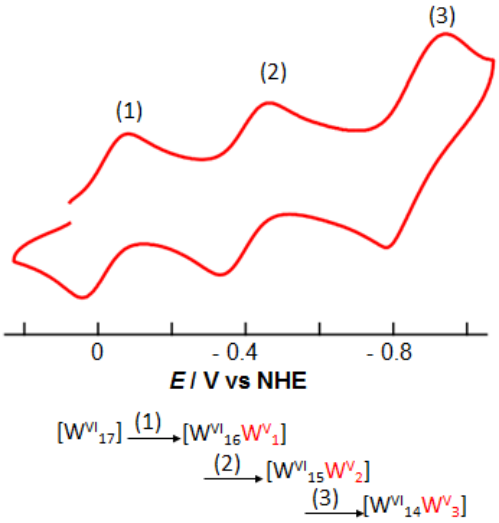

Figure 26. Solid state CV of 0.1 mM $[W_{17}(bza)_2]$ in DMF and $TBAPF_6$ as electrolyte. Scan rate: 0.1 $V \cdot s^{-1}$.

The more the cyclic voltammogram is shifted towards positive potentials, the easier it is to reduce the polyoxometalate due to a lower energy of the *lowest unoccupied molecular orbital* (LUMO), where the electrons that the POM gains when the reduction occurs are promoted to.

An important parameter that is obtained from the CV is the half wave potential ($E_{1/2}$) potential that is worked out from the average of the reduction and the oxidation semi potentials of each reversible redox process (**Eq. 6**).

$$E_{1/2}\ (V) = \frac{E(red) + E(ox)}{2} \qquad \textbf{(6)}$$

In **Fig. 27**, cyclic voltammogram of $[Bu_4N]_6[P_2W_{18}O_{62}]$ is showed and three reversible redox processes appear.

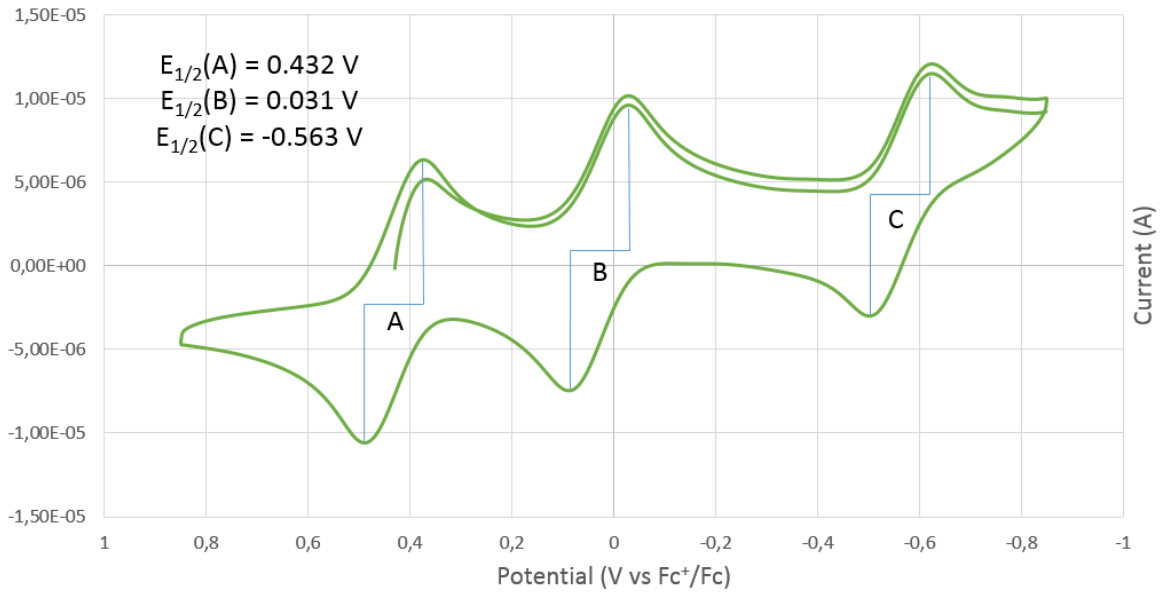

Figure 27. CV of 1 mM $[Bu_4N]_6[P_2W_{18}O_{62}]$ in DMF and $TBAPF_6$ as electrolyte. Scan rate: 0.1 $V \cdot s^{-1}$.

In **Fig. 28**, cyclic voltammogram of $[Bu_4N]_8H_2[P_2W_{17}O_{61}]$ is showed and two reversible redox processes appear.

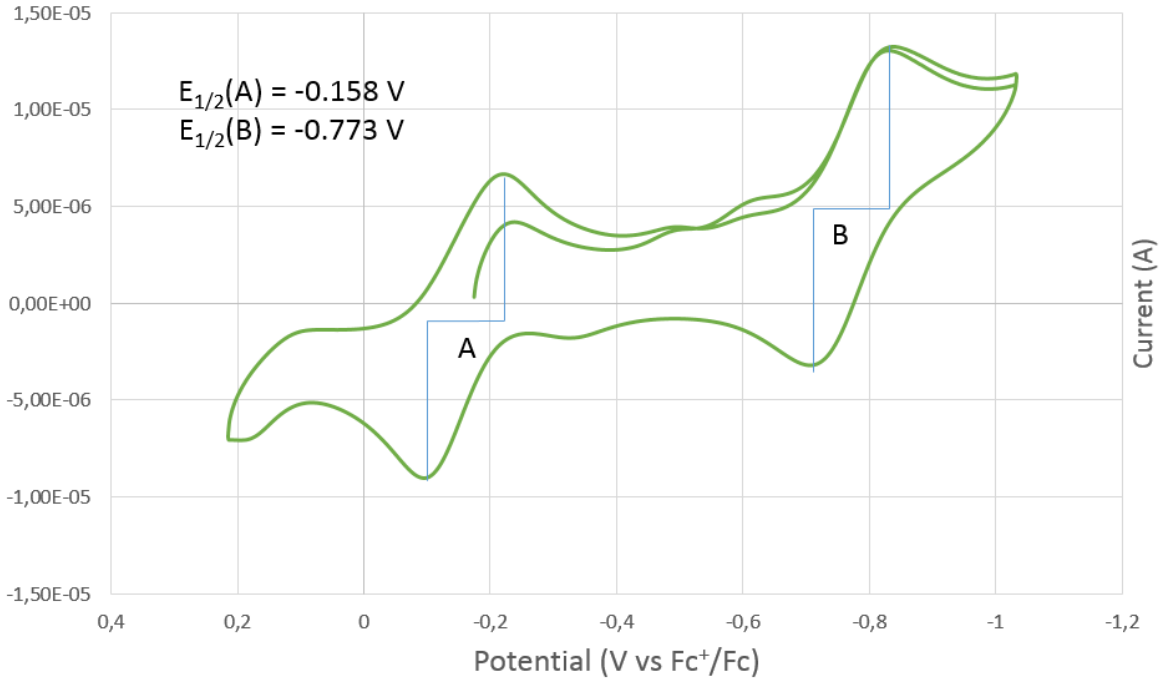

Figure 28. CV of 1 mM $[Bu_4N]_8H_2[P_2W_{17}O_{61}]$ in DMF and $TBAPF_6$ as electrolyte. Scan rate: 0.1 $V \cdot s^{-1}$.

In **Fig. 29**, cyclic voltammogram of $[Bu_4N]_5K[P_2W_{17}O_{57}(HPO_3)_2]$ is showed and four reversible redox processes appear.

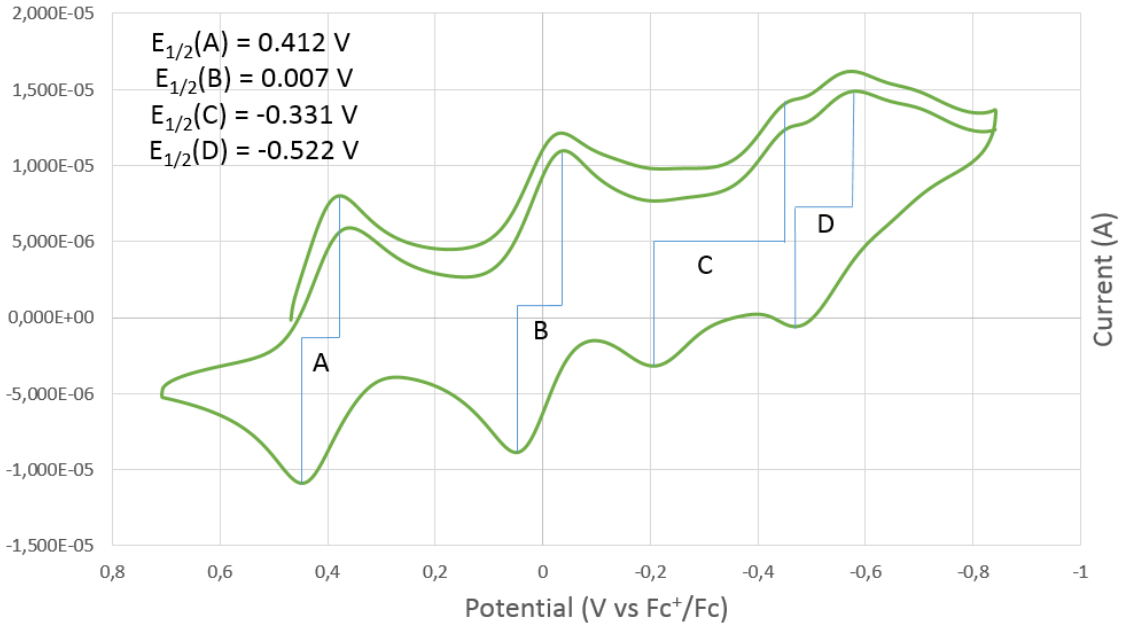

Figure 29. CV of 1 mM $[Bu_4N]_5K[P_2W_{17}O_{57}(HPO_3)_2]$ in DMF and $TBAPF_6$ as electrolyte. Scan rate: 0.1 $V \cdot s^{-1}$.

In **Fig. 30**, cyclic voltammogram of $[Bu_4N]_5K[P_2W_{17}O_{57}(HPO_4)_2]$ is showed and three reversible redox processes appear.

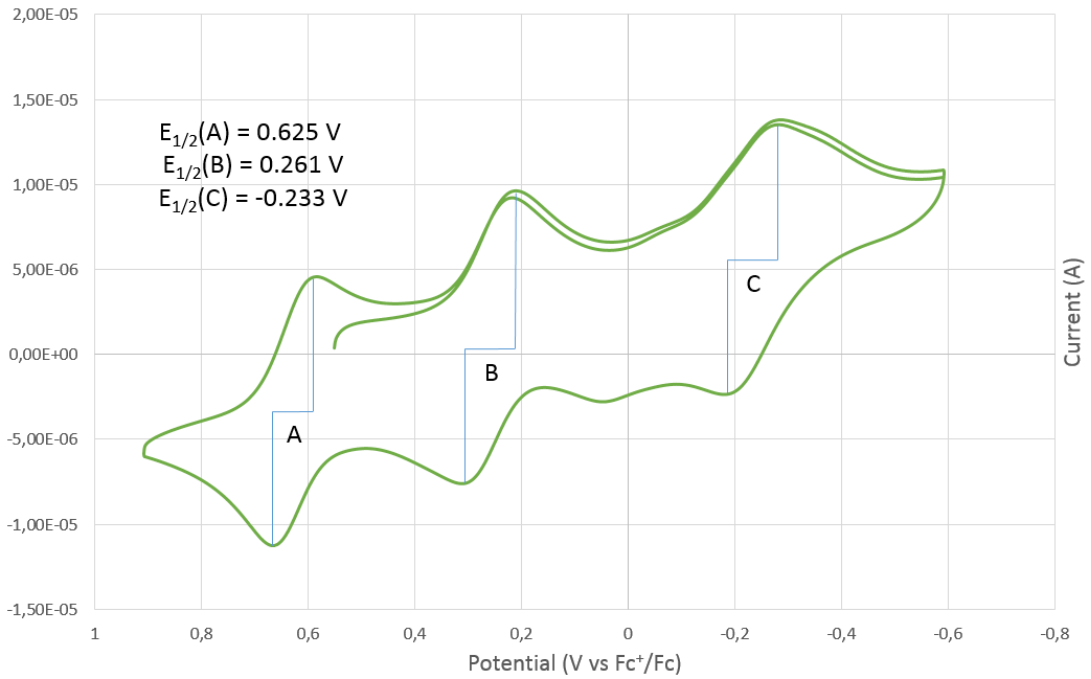

Figure 30. CV of 1 mM $[Bu_4N]_5K[P_2W_{17}O_{57}(HPO_4)_2]$ in DMF and $TBAPF_6$ as electrolyte. Scan rate: 0.1 $V \cdot s^{-1}$.

In **Fig. 31**, cyclic voltammograms of all the salts are showed.

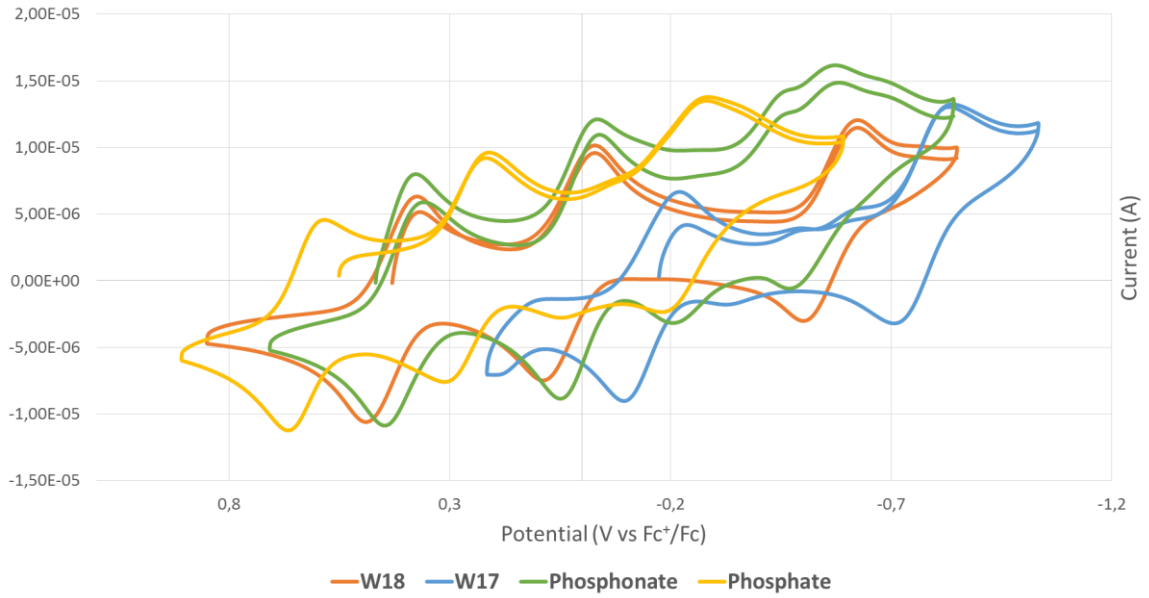

Figure 31. CV of 1 mM samples in DMF and $TBAPF_6$ as electrolyte. Scan rate: 0.1 $V \cdot s^{-1}$. *W18* stands for $[Bu_4N]_6[P_2W_{18}O_{62}]$, *W17* for $[Bu_4N]_8H_2[P_2W_{17}O_{61}]$, *Phosphonate* stands for $[Bu_4N]_5K[P_2W_{17}O_{57}(HPO_3)_2]$ and *Phosphate* for $[Bu_4N]_5K[P_2W_{17}O_{57}(HPO_4)_2]$.

What is showed in the superposition of all the CV's is that there is a shift of the data from the inorganic hybrids (*Phosphonate* and *Phosphate*) towards positive values. As stated above, this shift means that hybrids have lower LUMO energies and thus it is easier for the structure to incorporate electrons when the reduction occurs.

5.5. Ultraviolet-visible spectroscopy

Ultraviolet-visible spectroscopy (UV-Vis) is based on the fact that molecules containing π-electrons or non-bonding electrons can absorb the energy in the form of ultraviolet or visible light which excites these electrons into higher anti-bonding molecular orbitals. The more easily the electrons are excited (lower energy gap between the HOMO and the LUMO), the longer the wavelength of light the molecule can absorb.

The highest absorbance in polyoxometalates UV-Vis spectra corresponds to a ligand to metal charge transfer (LMCT). Oxo donor ligands transfer one electron from their *p* orbitals towards the tungsten *d* orbitals.

Fig. 32 below shows the overlaid UV-vis spectrum for the starting plenary and lacunary polyoxotungstates as well as for the inorganic hybrids in *N,N*-dimethylformamide (DMF).

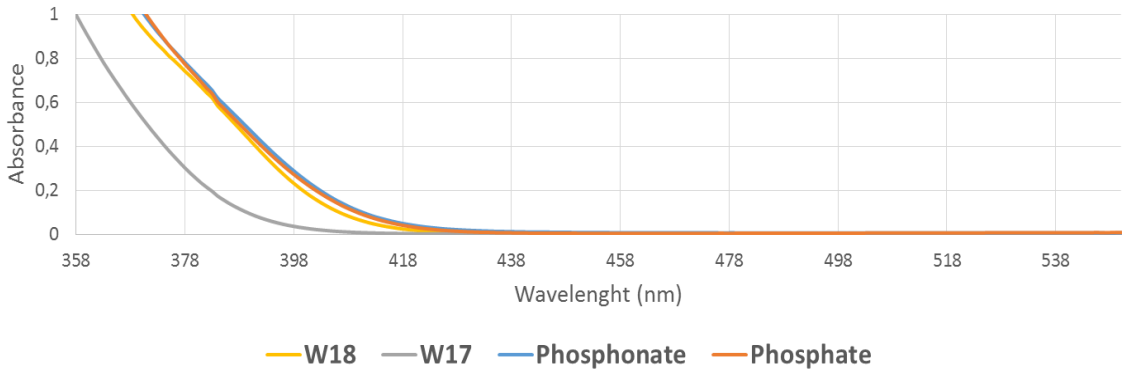

Figure 32. UV-Vis spectra of $[Bu_4N]_6[P_2W_{18}O_{62}]$ (*W18*), $[Bu_4N]_8H_2[P_2W_{17}O_{61}]$ (*W17*), $[Bu_4N]_5K[P_2W_{17}O_{57}(HPO_3)_2]$ (*Phosphonate*) and $[Bu_4N]_5K[P_2W_{17}O_{57}(HPO_4)_2]$ (*Phosphate*) in DMF at $5{\cdot}10^{-4}$ M concentration.

Table 5 summarises the key data including maximum absorption and extension coefficients, following Lambert-Beer law in **Eq. 7** where Abs is absorbance, C is the concentration, L is the cuvette length and finally ε is the extension coefficient.

$$Abs = C \cdot L \cdot \varepsilon \qquad \textbf{(7)}$$

Table 5. UV-Vis data for all the compounds.

	λ_{max} (nm)	ε_{max}
$[Bu_4N]_6[P_2W_{18}O_{62}]$	344	7404
$[Bu_4N]_8H_2[P_2W_{17}O_{61}]$	336	5657
$[Bu_4N]_5K[P_2W_{17}O_{57}(HPO_3)_2]$	344	7605
$[Bu_4N]_5K[P_2W_{17}O_{57}(HPO_4)_2]$	347	6468

The phosphonate hybrid material shows increased absorption compared to all the other compounds, which can be seen from the molar extinction coefficient values. The peaks observed are because of LMCT phenomenon, as previously discussed.

6. Conclusions and future work

After the realisation of this project, and based on the initial objectives, several conclusions have been reached:

- The synthesis of the inorganic hybrid polyoxotungstates, $[Bu_4N]_5K[P_2W_{17}O_{57}(HPO_3)_2]$ and $[Bu_4N]_5K[P_2W_{17}O_{57}(HPO_4)_2]$, has been successfully achieved and a procedure has been established
- The inorganic hybrids perform a shift in the cyclic voltammograms towards positive potentials and this means their photoactivity properties are better than those for the starting materials, the Wells-Dawson polyoxotungstate and its lacunary structure. This hybrids can be more easily reduced because of lower LUMO energies and thus, interesting applications may arise from this property.
- The reactivity of the phosphonate group in a polyoxotungstate environment has been slightly studied by performing several reactions in different conditions, such as time, temperature and light.

Further work needs to be done in order to improve the synthetic procedure for both hybrids materials as some impurities still remain on both cases, though more abundant in $[Bu_4N]_5K[P_2W_{17}O_{57}(HPO_4)_2]$. Regarding the organofunctionalisation of the hybrids, as it has not been successful by far, it requires further study and efforts.

7. Bibliography

(1) Dolbecq, A.; Dumas, E.; Mayer, C. R.; Mialane, P. *Chem. Rev.* **2010**, *110*, 6009–6048.

(2) Pope, M. T.; Müller, A. *Angew. Chemie Int. Ed. English* **1991**, *30* (1), 34–48.

(3) Pope, M. T. *Heteropoly and Isopoly Oxometalates*, WILEY-VCH.; Berlín, 1983.

(4) López, X.; Bo, C.; Poblet, J.-M.; Sarasa, J. P. *Inorg. Chem.* **2003**, *42* (8), 2634–2638.

(5) Proust, A.; Thouvenot, R.; Gouzerh, P.; Gómez-García, C. J.; Roth, J.; Khitrov, G. A.; Marshall, A. G.; Sarkar, S.; Bud'ko, S.; Harrison, N.; Zhou, Y.; Zhang, L.; Musaev, D. G.; Geletii, Y. V. *Chem. Commun.* **2008**, *154* (16), 1837–1840.

(6) Miras, H. N.; Vilà-Nadal, L.; Cronin, L.; Cronin, L.; Akutagawa, T.; Nakamura, T.; Scandurra, A.; Pignataro, B.; Gadegaard, N.; Cronin, L.; Cronin, L.; Dolbecq, A. *Chem. Soc. Rev.* **2014**, *43* (16), 5679–5699.

(7) Long, D.-L.; Tsunashima, R.; Cronin, L. *Angew. Chemie Int. Ed.* **2010**, *49* (10), 1736–1758.

(8) Jeannin, Y. P. *Chem. Rev.* **1998**, *98* (1), 51–76.

(9) Becker, G.; Schmidt, H.; Uhl, G.; Uhl, W.; Regitz, M.; Rösch, W.; Vogelbacher, U.-J. *Inorganic Syntheses*; 2007; Vol. 27.

(10) Saikat Mandal; PR. Selvakannan; Renu Pasricha, A.; Sastry*, M. *J. Am. Chem. Soc.* **2003**, *125* (28), 8440–8441.

(11) Wang, S.-S.; Yang, G.-Y. *Chem. Rev.* **2015**, *115* (11), 4893–4962.

(12) Lv, H.; Geletii, Y. V.; Zhao, C.; Vickers, J. W.; Zhu, G.; Luo, Z.; Song, J.; Lian, T.; Musaev, D. G.; Hill, C. L.; Odobel, F.; Lian, T.; Marcaccio, M.; Scorrano, G.; Scoles, G.; Paolucci, F.; Prato, M.; Bonchio, M.; Norimatsu, T.; Norreys, P. A.; Sakabe, S.; Tanaka, K. A.; Youssef, A.; Zepf, M.; Yamanaka, T. *Chem. Soc. Rev.* **2012**, *41* (22), 7572–7589.

(13) Zhu, Z.; Tain, R.; Rhodes, C. *Can. J. Chem.* **2003**, *81* (10), 1044–1050.

(14) Sadakane, M.; Steckhan, E. *Chem. Rev.* **1998**, *98* (1), 219–225.

(15) Hill, C. L. *J. Mol. Catal. A Chem.* **2007**, *262* (1–2), 2–6.

(16) Jeffrey T. Rhule; Craig L. Hill, * and; Judd, D. A.; Schinazi*, R. F. *Chem. Commun.* **1998**, *98*, 327–357.

(17) Zhou, M.; Guo, L.; Lin, F.; Liu, H. *Anal. Chim. Acta* **2007**, *587* (1), 124–131.

(18) Rüther, T.; Hultgren, V. M.; Timko, B. P.; Bond, A. M.; William R. Jackson, A.; Wedd, A. G. *J. Am. Chem. Soc.* **2003**, *125* (33), 10133–10143.

(19) Streb, C.; Long, D. L.; Miras, H. N.; Gabb, D.; Pradeep, C. P.; Cronin, L.; Simonetti, A.; Burns, P. C.; Kozik, M.; Musaev, D. G.; Hill, C. L.; Lian, T. Q. *Dalt. Trans.* **2012**, *41* (6), 1651–1659.

(20) Yihang Guo; Yuanhong Wang; Changwen Hu, *; Yonghui Wang, A.; Wang, E.; And, Y. Z.; Feng*, S. *Chem. Mater.* **2000**, *12* (11), 3501–3508.

(21) Clemente-Juan, J. M.; Coronado, E. *Coord. Chem. Rev.* **1999**, *193–195*, 363.

(22) Mizuno, N.; Yamaguchi, K.; Kamata, K. *Coord. Chem. Rev.* **2005**, *249*, 1944–1956.

(23) He, T.; Yao, J. *Prog. Mater. Sci.* **2006**, *51* (6), 810–870.

(24) Kögerler, P.; Tsukerblat, B.; Müller, A.; Luban, M.; Kögerler, P.; Schmidtmann, M.; Talismanov, S. S.; Luban, M.; Krickemeyer, E.; Müller, A.; Qiu, Y.; Exler, M.; Schnack, J.; Luban, M. *Dalt. Trans.* **2010**, *39* (1), 21–22.

(25) Xu, B.; Lu, M.; Kang, J.; Wang, D.; Brown, J.; Peng, Z. *Chem. Mater.* **2005**, *17* (11), 2841.

(26) Gómez-Romero, P.; Lira-Cantú, M. *Adv. Mater.* **1997**, *9* (2), 144–147.

(27) Varga, G. M.; Papaconstantinou, E.; Pope, M. T. *Inorg. Chem.* **1970**, *9* (3), 662–667.

(28) Moore, A. R.; Kwen, H.; Beatty, A. M.; Maatta, E. A.; Rheingold, A. L.; Thouvenot, R.; Gouzerh, P.; Maatta, E. A. *Chem. Commun.* **2000**, *122* (18), 1793–1794.

(29) Mayer, C. R.; Thouvenot, R.; Lalot*, T. *Macromolecules* **2000**, *33* (12), 4433.

(30) Graham, C. R.; Finke, R. G. *Inorg. Chem.* **2008**, *47* (9), 3679–3686.

(31) Lyon, D. K.; Miller, W. K.; Novet, T.; Domaille, P. J.; Evitt, E.; Johnson, D. C.; Finke, R. G. *Am. Chem. Soc.* **1991**, *113* (19), 7209–7221.

(32) Bartis, J.; Sukal, S.; Dankova, M.; Kraft, E.; Kronzon, R.; Blumenstein, M.; Francesconi, L. C. *J. Chem. Soc. Trans.* **1997**, No. 11, 1937–1944.